Integral equation approach to time-dependent kinematic dynamos in finite domains

Mingtian Xu,* Frank Stefani,† and Gunter Gerbeth‡
Forschungszentrum Rossendorf, P.O. Box 510119, D-01314 Dresden, Germany
(Received 19 June 2003; revised manuscript received 16 December 2003; published 16 November 2004)

The homogeneous dynamo effect is at the root of cosmic magnetic field generation. With only a very few exceptions, the numerical treatment of homogeneous dynamos is carried out in the framework of the differential equation approach. The present paper tries to facilitate the use of integral equations in dynamo research. Apart from the pedagogical value to illustrate dynamo action within the well-known picture of the Biot-Savart law, the integral equation approach has a number of practical advantages. The first advantage is its proven numerical robustness and stability. The second and perhaps most important advantage is its applicability to dynamos in arbitrary geometries. The third advantage is its intimate connection to inverse problems relevant not only for dynamos but also for technical applications of magnetohydrodynamics. The paper provides the first general formulation and application of the integral equation approach to time-dependent kinematic dynamos, with stationary dynamo sources, in finite domains. The time dependence is restricted to the magnetic field, whereas the velocity or corresponding mean-field sources of dynamo action are supposed to be stationary. For the spherically symmetric α^2 dynamo model it is shown how the general formulation is reduced to a coupled system of two radial integral equations for the defining scalars of the poloidal and toroidal field components. The integral equation formulation for spherical dynamos with general stationary velocity fields is also derived. Two numerical examples—the α^2 dynamo model with radially varying α and the Bullard-Gellman model—illustrate the equivalence of the approach with the usual differential equation method. The main advantage of the method is exemplified by the treatment of an α^2 dynamo in rectangular domains.

DOI: 10.1103/PhysRevE.70.056305 PACS number(s): 47.65.+a, 52.65.Kj, 91.25.Cw

I. INTRODUCTION

Cosmic magnetic fields, including the fields of planets, stars, and galaxies, result from the hydromagnetic dynamo effect [1,2]. The last decades have seen tremendous progress in the analytical and numerical treatment of magnetic field generation in cosmic bodies. Recently, the hydromagnetic dynamo effect has been validated experimentally in large liquid sodium facilities in Riga and Karlsruhe [3–7].

The usual way to treat hydromagnetic dynamos numerically is within the differential equation approach. Supposing the fluid velocity $\mathbf{u}$ to be given, the governing differential equation is the induction equation for the magnetic field $\mathbf{B}$,

$$\frac{\partial \mathbf{B}}{\partial t} = \boldsymbol{\nabla} \times (\mathbf{u} \times \mathbf{B}) + \frac{1}{\mu_0 \sigma} \Delta \mathbf{B}, \tag{1}$$

with μ_0 and σ denoting the permeability of the free space and the electrical conductivity of the fluid, respectively. Equation (1) follows directly from pre-Maxwell's equations and Ohm's law in moving conductors. Note that the magnetic field has to be divergence free:

$$\boldsymbol{\nabla} \cdot \mathbf{B} = 0. \tag{2}$$

In the case of vanishing excitations of the magnetic field from outside the considered finite region, the boundary condition for the magnetic field reads

$$\mathbf{B} = \mathbf{O}(r^{-3}) \quad \text{as} \quad r \to \infty. \tag{3}$$

The induction equation (1) is sufficient to treat *kinematic dynamo models* in which the backreaction of the self-excited magnetic field on the flow is neglected. Such a simplification is justified during the initial phase of self-excitation when the magnetic field is weak. For stronger fields, one has to cope with *dynamically consistent dynamo models* which require the simultaneous solution of the induction equation for the magnetic field and the Navier-Stokes equation for the velocity. This saturation regime, however, will not be considered in the present paper.

The spherical geometry of many cosmic bodies such as planets and stars has simplified dynamo simulations in one important respect: for the spherical case the boundary conditions for the magnetic field can be reformulated separately for every degree and order of the spherical harmonics, which makes any particular treatment of the magnetic fields in the exterior superfluous.

When it comes to dynamos in other than spherical geometries, this pleasant situation changes. Then the correct handling of the nonlocal boundary conditions becomes nontrivial. Such a problem appears, e.g., in the numerical simulation of the recent dynamo experiments that are of cylindrical shape, but also in the simulations of galactic dynamos. There are some ways to cope with this problem: one can use simplified local boundary conditions ("vertical field condition") [8,9], one can embed the actual dynamo body into a sphere with the region between the actual dynamo and the surface of the sphere virtually filled with a medium of lower electrical conductivity [10,11], or one can solve the Laplace equation in the exterior and fit the solution at the boundary to the solution in the interior [12], which is, how-

*Electronic address: M.Xu@fz-rossendorf.de
†Electronic address: F.Stefani@fz-rossendorf.de
‡Electronic address: G.Gerbeth@fz-rossendorf.de

ever, a tedious and time-consuming procedure. Note that the application of local boundary conditions is usually paid with a considerable loss of accuracy. For example, for the sake of comparison we have applied the simplified vertical field conditions for the simulation of the Riga dynamo experiment and found, for the critical magnetic Reynolds number, a deviation of about 15% from the correct value.

The integral equation approach that we will establish in the present paper is intended to change this unsatisfactory situation concerning the handling of boundary conditions. For the steady case and for infinite domains of homogeneous conductivity, the integral equation approach was used in a few previous papers [13–16]. The inclusion of boundaries, again for the steady case, was already delineated in the book of Roberts [17]. In Roberts' own opinion ([17], p. 74), however, this formulation did "… not appear, in general, to be very useful." In [18] we have tried to put this pessimistic judgment into question. In particular, we have derived from the general theory a system of one-dimensional integral equations for a dynamo model with a spherically symmetric, isotropic helical turbulence parameter α in a finite sphere, and we have rederived analytically the solution found by Krause and Steenbeck [19] for the special case of constant α. In [20] we have investigated the performance of numerical schemes to solve these integral equations for steady α^2 dynamos.

It should be pointed out that for the steady case a similar approach had been established earlier under the label "velocity-current-formulation" by Meir and Schmidt [21,22]. This approach had also the pronounced aim to circumvent the numerical treatment outside the region of interest. However, the numerical focus of this work laid more on steady, coupled magnetohydrodynamic (MHD) problems with small magnetic Reynolds number than on dynamo problems.

In the present paper, we generalize the integral equation approach for steady dynamos in finite domains to dynamos with time-dependent magnetic fields. Note that in the following "time-dependent" will only refer to the magnetic field, whereas the dynamo source is always supposed to be stationary. Such a formulation is highly requested for a number of problems that are related to the data analysis for the existing and to the optimization of future dynamo experiments. For example, in connection with the Riga dynamo experiment there is the urgent need for an inverse problem solver in order to reconstruct, from the wealth of measured magnetic field data, the Lorentz force influenced sodium flow in the saturation regime [23]. An efficient forward problem solver, based on the integral equation approach, could represent an essential ingredient of such an inverse problem solver. Further applications are foreseeable in metallurgy and crystal growth where a contactless determination of the flow velocity, based on the external measurement of induced magnetic fields, would be highly desirable. There has been some theoretical and experimental progress towards such a contactless inductive flow measuring technique [24–27]. Presently, the underlying inversion technique calls for its generalization to time-dependent magnetic fields in order to mitigate the remaining nonuniqueness which concerns the depth dependence of the reconstructed velocity field.

There are various possibilities for the concrete formulation of the integral equation approach. Here, in contrast to earlier statements on this matter [16] that the use of the Green's function of the Helmholtz equation will lead to a nonlinear eigenvalue equation, we present a linear formulation of the eigenvalue problem. This makes the approach more attractive for numerical treatment and, hence, represents an essential step for its applicability.

For the paradigmatic case of a time-dependent spherically symmetric, isotropic α^2 dynamo we derive, starting from the general formulation, a coupled system of two radial integral equations which is solved numerically. The equivalence with the results of a differential equation solver is made evident. We also derive the coupled system of radial integral equations for spherical dynamos with general velocity fields and treat numerically the well-known Bullard-Gellman model within the new approach.

These examples in spherical geometry demonstrate the equivalence of the integral equation approach with the differential equation approach. The main advantage of the former—its suitability for handling dynamo problems in arbitrary domains—will then be exemplified by the treatment of a simple dynamo in rectangular geometry. Extending our recent work on steady α^2 dynamos in such domains [20] to the time-dependent case, we compute the growth rates and the eigenfields in dependence on α and compare them with the corresponding results for a spherical domain. First, we find that the free decay is faster than in the spherical case. However, for increasing α the growth rates of the leading eigenmode of the cubic and "matchbox" dynamo both converge to that of the spherical case. This is a physically interesting result indicating that the boundary effects become less important with increasing α.

II. GENERAL FORMULATION

Assume a stationary velocity field or a corresponding mean-field dynamo source, acting in a finite domain D with a boundary S, surrounded by nonconducting space. For this setting, we will derive the general form of the integral equation approach for time-dependent magnetic fields, generalizing the basic idea and the methods from the steady case [18,20].

We start with the pre-Maxwell's equations (the displacement current can be skipped in the quasistationary approximation)

$$\nabla \times \mathbf{E}(\mathbf{r},t) = -\frac{\partial \mathbf{B}(\mathbf{r},t)}{\partial t}, \tag{4}$$

$$\nabla \cdot \mathbf{B}(\mathbf{r},t) = 0, \tag{5}$$

$$\nabla \times \mathbf{B}(\mathbf{r},t) = \mu_0 \mathbf{j}(\mathbf{r},t), \tag{6}$$

where $\mathbf{B}(\mathbf{r},t)$ is the magnetic field, $\mathbf{E}(\mathbf{r},t)$ the electric field, $\mathbf{r}$ the position vector, t the time, and μ_0 the magnetic permeability of the free space. The current density $\mathbf{j}(\mathbf{r},t)$ satisfies Ohm's law

$$\mathbf{j}(\mathbf{r},t) = \sigma[\mathbf{E}(\mathbf{r},t) + \mathbf{F}(\mathbf{r},t)] \tag{7}$$

inside the dynamo domain D, and it vanishes outside D. $\mathbf{F}(\mathbf{r},t)$ denotes the electromotive force (emf) $\mathbf{u}(\mathbf{r})\times\mathbf{B}(\mathbf{r},t)$, where $\mathbf{u}(\mathbf{r})$ is the velocity of the fluid motion, which we suppose to be stationary. In the framework of mean-field electrodynamics (see, e.g., [1]) $\mathbf{B}(\mathbf{r},t)$, $\mathbf{j}(\mathbf{r},t)$, and $\mathbf{F}(\mathbf{r},t)$, are split into mean fields and fluctuating fields. Then $\mathbf{F}(\mathbf{r},t)$ can be fixed to the form

$$\mathbf{F}(\mathbf{r},t) = \mathbf{u}(\mathbf{r}) \times \mathbf{B}(\mathbf{r},t) + \alpha(\mathbf{r})\mathbf{B}(\mathbf{r},t) - \beta(\mathbf{r})\,\boldsymbol{\nabla} \times \mathbf{B}(\mathbf{r},t), \tag{8}$$

where $\mathbf{u}(\mathbf{r})$ and $\mathbf{B}(\mathbf{r},t)$ now denote the mean velocity and the mean magnetic field, respectively. The term $\alpha(\mathbf{r})\mathbf{B}(\mathbf{r},\mathbf{t})$ describes the emf due to the nonmirrorsymmetric part of the turbulence (α effect), and the term $\beta(\mathbf{r})\boldsymbol{\nabla}\times\mathbf{B}(\mathbf{r},t)$ describes another effect which can be interpreted as a conductivity decrease due to the turbulence (β effect).

The equations given so far, together with initial conditions for $\mathbf{B}$, define an initial value problem for $\mathbf{B}(\mathbf{r},t)$ which can be combined into the form of Eq. (1). Together with the requirements that there be no surface currents on S and that $\mathbf{B}(\mathbf{r},t)$ vanish at infinity, they allow one to determine $\mathbf{B}(\mathbf{r},t)$ once the concrete dependence of $\mathbf{F}(\mathbf{r},t)$ on $\mathbf{B}(\mathbf{r},t)$ has been fixed.

Under the condition that $\mathbf{u}$, α, and β in Eq. (8) only depend on the position $\mathbf{r}$, we can search for modal solutions of the form

$$\mathbf{E}(\mathbf{r},t) = \mathbf{E}(\mathbf{r})e^{\lambda t}, \quad \mathbf{B}(\mathbf{r},t) = \mathbf{B}(\mathbf{r})e^{\lambda t}, \quad \mathbf{F}(\mathbf{r},t) = \mathbf{F}(\mathbf{r})e^{\lambda t},$$
$$\mathbf{j}(\mathbf{r},t) = \mathbf{j}(\mathbf{r})e^{\lambda t}, \tag{9}$$

where λ is in general a complex constant. Then Maxwell's equations and Ohm's law transform into

$$\boldsymbol{\nabla} \times \mathbf{E} = -\lambda\mathbf{B}, \tag{10}$$

$$\boldsymbol{\nabla} \cdot \mathbf{B} = 0, \tag{11}$$

$$\boldsymbol{\nabla} \times \mathbf{B} = \mu_0\mathbf{j}, \tag{12}$$

$$\mathbf{j} = \sigma(\mathbf{E} + \mathbf{F}). \tag{13}$$

Hereafter, the symbols $\mathbf{B}$, $\mathbf{E}$, $\mathbf{j}$, and $\mathbf{F}$ denote the functions which only depend on the position $\mathbf{r}$, but not on the time t.

Taking the curl of Eq. (10) and employing Eqs. (12) and (13), we obtain the eigenvalue problem

$$\lambda\mathbf{B} = \boldsymbol{\nabla} \times (\mathbf{u} \times \mathbf{B}) + \frac{1}{\mu_0\sigma}\Delta\mathbf{B} =: \mathcal{L}\mathbf{B}, \tag{14}$$

with the complex eigenfrequency λ, implying exponential growth of $\mathbf{B}$ with the rate $\mathrm{Re}(\lambda)$.

An important point should be mentioned here that concerns the intricate relation of the time-dependent solutions of Eq. (1) and the time evolution of the eigenfunctions of Eq. (14). The fact that the operator $\mathcal{L}$ on the right-hand side (RHS) of Eq. (14) is, in general, non-normal—i.e., $\mathcal{L}\mathcal{L}^\dagger \neq \mathcal{L}^\dagger\mathcal{L}$—implies that Eq. (14) does not in general have orthogonal eigenvectors, and the solution of the original time-dependent induction equation (1) can show transient growth even in the case that all individual eigenvalues of Eq. (14) have negative real parts [28–30].

However, for $t\to\infty$, the time evolution of the magnetic field is still governed by the eigenvalue with the largest real part. The determination of other than the leading eigenvalue might also be important to understand qualitative spectral changes, like that from steady to oscillatory behavior [31]. We are convinced that, despite the recent achievements in the understanding of transient growth for non-normal operators, there is still room for a modal analysis of the induction equation. This applies, in particular, to the correct handling of dynamos in nonspherical domains, which is the main focus of this paper.

Since the magnetic field $\mathbf{B}$ is divergence free, there exists a magnetic vector potential $\mathbf{A}(\mathbf{r})$ such that

$$\mathbf{B} = \boldsymbol{\nabla} \times \mathbf{A}, \tag{15}$$

which implies, together with Eq. (10), that

$$\boldsymbol{\nabla} \times (\mathbf{E} + \lambda\mathbf{A}) = 0. \tag{16}$$

Therefore, $\mathbf{E}+\lambda\mathbf{A}$ has to be irrotational, and we can write

$$\mathbf{E} + \lambda\mathbf{A} = -\,\boldsymbol{\nabla}\varphi. \tag{17}$$

Subsequently, Ohm's law gets the form

$$\mathbf{j} = \sigma(\mathbf{F} - \lambda\mathbf{A} - \boldsymbol{\nabla}\varphi). \tag{18}$$

In the following, we will derive a system of integral equations that is equivalent to the differential equation formulation (14). The starting point for the first integral equation is the application of the Biot-Savart law on Eq. (12), leading to

$$\mathbf{B}(\mathbf{r}) = \frac{\mu_0}{4\pi}\int_D \frac{\mathbf{j}(\mathbf{r}') \times (\mathbf{r} - \mathbf{r}')}{|\mathbf{r} - \mathbf{r}'|^3} dV'. \tag{19}$$

It is well known that the *curl* operator in Eq. (12) is a left inverse of the Biot-Savart operator when the current $\mathbf{j}$ is divergence free and tangent to the boundary of the domain [32]. Both conditions are indeed fulfilled in our case. Inserting Eq. (18) into Eq. (19) and using Gauss's theorem, we get the first integral equation

$$\mathbf{B}(\mathbf{r}) = \frac{\mu_0\sigma}{4\pi}\int_D \frac{\mathbf{F}(\mathbf{r}') \times (\mathbf{r} - \mathbf{r}')}{|\mathbf{r} - \mathbf{r}'|^3} dV' - \frac{\mu_0\sigma\lambda}{4\pi}\int_D \frac{\mathbf{A}(\mathbf{r}') \times (\mathbf{r} - \mathbf{r}')}{|\mathbf{r} - \mathbf{r}'|^3} dV' - \frac{\mu_0\sigma}{4\pi}\int_S \varphi(\mathbf{s}')\mathbf{n}(\mathbf{s}') \times \frac{\mathbf{r} - \mathbf{s}'}{|\mathbf{r} - \mathbf{s}'|^3} dS', \tag{20}$$

with $\mathbf{n}(\mathbf{s}')$ denoting the outward directed unit vector at the boundary point $\mathbf{s}'$ and dS' denoting an area element at this point. For some purposes it might be useful to express the volume integrals in Eq. (20) in the form

$$\int_D \frac{\mathbf{F}(\mathbf{r}')\times(\mathbf{r}-\mathbf{r}')}{|\mathbf{r}-\mathbf{r}'|^3}dV' = \int_D \frac{\nabla_{r'}\times\mathbf{F}(\mathbf{r}')}{|\mathbf{r}-\mathbf{r}'|}dV' - \int_S \mathbf{n}(\mathbf{s}') \times \frac{\mathbf{F}(\mathbf{s}')}{|\mathbf{r}-\mathbf{s}'|}dS', \tag{21}$$

and, using $\nabla\times\mathbf{A}=\mathbf{B}$,

$$\int_D \frac{\mathbf{A}(\mathbf{r}')\times(\mathbf{r}-\mathbf{r}')}{|\mathbf{r}-\mathbf{r}'|^3}dV' = \int_D \frac{\mathbf{B}(\mathbf{r}')}{|\mathbf{r}-\mathbf{r}'|}dV' - \int_S \mathbf{n}(\mathbf{s}') \times \frac{\mathbf{A}(\mathbf{s}')}{|\mathbf{r}-\mathbf{s}'|}dS'. \tag{22}$$

For the steady case ($\lambda=0$) Eq. (20) reduces to the form given in [18], with one volume integral over **B** and one boundary integral over φ. The latter one would vanish only in the case that the dynamo region is extended to infinity. The time dependence introduces now a new volume integral over the vector potential **A** or another volume integral over **B** and one boundary integral over **A** which cannot be reduced to a simple expression in **B**. Before we focus on this point, let us first derive the integral equation for φ.

From Eq. (18) and the demand that the current has to be divergence free, $\nabla\cdot\mathbf{j}=0$, we get a Poisson equation for φ:

$$\Delta\varphi = \nabla\cdot(\mathbf{F}-\lambda\mathbf{A}). \tag{23}$$

Assuming a vacuum boundary condition which means that the current must not leave the domain D, we obtain from Green's theorem the following boundary integral equation for φ:

$$p\ \varphi(\mathbf{r}) = \frac{1}{4\pi}\int_D \frac{\mathbf{F}(\mathbf{r}')\cdot(\mathbf{r}-\mathbf{r}')}{|\mathbf{r}-\mathbf{r}'|^3}dV' - \frac{\lambda}{4\pi}\int_D \frac{\mathbf{A}(\mathbf{r}')\cdot(\mathbf{r}-\mathbf{r}')}{|\mathbf{r}-\mathbf{r}'|^3}dV' - \frac{1}{4\pi}\int_S \varphi(\mathbf{s}')\mathbf{n}(\mathbf{s}')\cdot\frac{\mathbf{r}-\mathbf{s}'}{|\mathbf{r}-\mathbf{s}'|^3}dS', \tag{24}$$

where $p=1$ for points **r** inside D, $p=1/2$ for points $\mathbf{r}=\mathbf{s}$ on S, and $p=0$ for points **r** outside D. Again, other expressions of the volume integrals might be useful:

$$\int_D \frac{\mathbf{F}(\mathbf{r}')\cdot(\mathbf{r}-\mathbf{r}')}{|\mathbf{r}-\mathbf{r}'|^3}dV' = -\int_D \frac{\nabla\cdot\mathbf{F}(\mathbf{r}')}{|\mathbf{r}-\mathbf{r}'|}dV' + \int_S \mathbf{n}(\mathbf{s}')\cdot\frac{\mathbf{F}(\mathbf{s}')}{|\mathbf{r}-\mathbf{s}'|}dS', \tag{25}$$

$$\int_D \frac{\mathbf{A}(\mathbf{r}')\cdot(\mathbf{r}-\mathbf{r}')}{|\mathbf{r}-\mathbf{r}'|^3}dV' = -\int_D \frac{\nabla\cdot\mathbf{A}(\mathbf{r}')}{|\mathbf{r}-\mathbf{r}'|}dV' + \int_S \mathbf{n}(\mathbf{s}')\cdot\frac{\mathbf{A}(\mathbf{s}')}{|\mathbf{r}-\mathbf{s}'|}dS'. \tag{26}$$

If we use the Coulomb gauge for the vector potential, $\nabla\cdot\mathbf{A}=0$, we see that the volume integral in Eq. (26) vanishes.

For the steady case, Eqs. (20) and (24) with $\lambda=0$ are sufficient to determine the magnetic field **B**. But for the time-dependent case presently under consideration, we have to introduce the vector potential **A**, at least at the boundary, for completely formulating the problem. Necessarily we have to establish another relation for **A** in order to make the problem solvable. From Eq. (15) and Helmholtz's theorem ([33], p. 53) we can express the vector potential in one of the two forms

$$\mathbf{A}(\mathbf{r}) = \frac{1}{4\pi}\int_D \frac{\nabla_{r'}\times\mathbf{B}(\mathbf{r}')}{|\mathbf{r}-\mathbf{r}'|}dV' = \frac{1}{4\pi}\int_D \frac{\mathbf{B}(\mathbf{r}')\times(\mathbf{r}-\mathbf{r}')}{|\mathbf{r}-\mathbf{r}'|^3}dV' + \frac{1}{4\pi}\int_S \mathbf{n}(\mathbf{s}') \times \frac{\mathbf{B}(\mathbf{s}')}{|\mathbf{r}-\mathbf{s}'|}dS'. \tag{27}$$

The integral equations (20), (24), and (27) provide another complete formulation of the problem for **B**. The main advantage of this formulation is that one can avoid any treatment of fields in the exterior of D. The boundary conditions are being fulfilled by solving the additional integral equations for φ and **A**.

III. TEST CASE OF TIME-DEPENDENT SPHERICAL α^2 DYNAMOS

A. Radial integral equation system

In this section, we exemplify the general integral equation approach by applying it to a simple mean-field dynamo model with a spherically symmetric, isotropic helical turbulence parameter α. In contrast to the original model with constant α [1,19], whose advantage is the possibility of an analytical treatment, we allow here α to vary with radial coordinate r. After giving some definitions, we will obtain two coupled radial integral equations which will be used in the next subsection for numerical treatment. Note that for the steady case the corresponding derivation had been published in [18].

As usual in dynamo theory, we split the divergence-free magnetic field **B** into a poloidal and a toroidal part, denoted by $\mathbf{B}_P$ and $\mathbf{B}_T$. Since we use the Coulomb gauge $\nabla\cdot\mathbf{A}=0$, an equivalent decomposition can also be applied to the vector potential $\mathbf{A}=\mathbf{A}_P+\mathbf{A}_T$. We represent these fields by the defining scalars S, T, S^A, T^A according to

$$\mathbf{B}_P = \nabla\times\nabla\times\left(\frac{S}{r}\mathbf{r}\right), \quad \mathbf{B}_T = \nabla\times\left(\frac{T}{r}\mathbf{r}\right), \tag{28}$$

$$\mathbf{A}_P = \nabla\times\nabla\times\left(\frac{S^A}{r}\mathbf{r}\right), \quad \mathbf{A}_T = \nabla\times\left(\frac{T^A}{r}\mathbf{r}\right). \tag{29}$$

We introduce spherical coordinates r,θ,ϕ and denote the radius vector by **r**. The defining scalars and the electric potential are expanded in series of spherical harmonics $Y_{lm}(\theta,\phi)$—for example,

$$S(r,\theta,\phi)=\sum_{l,m} s_{lm}(r)Y_{lm}(\theta,\phi), \tag{30}$$

and corresponding expressions for $T(r,\theta,\phi)$, $S^A(r,\theta,\phi)$, $T^A(r,\theta,\phi)$, and $\varphi(r,\theta,\phi)$, in which $s_{lm}(r)$ are replaced by $t_{lm}(r)$, $s^A_{lm}(r)$, $t^A_{lm}(r)$, and $\varphi_{lm}(r)$, respectively.

For the spherical harmonics $Y_{lm}(\theta,\phi)$ the definition

$$Y_{lm}(\theta,\phi)=\sqrt{\frac{2l+1}{4\pi}\frac{(l-m)!}{(l+m)!}}\,P_{lm}(\cos\,\theta)e^{im\phi} \tag{31}$$

is employed, with P_{lm} denoting associated Legendre polynomials. The summations in Eq. (30) are over all degrees l and orders m satisfying $l\geqslant 0$ and $|m|\leqslant l$; terms with $l=0$, however, are without interest in the following. Since S, T, S^A, T^A, and φ are real, we have $s_{l-m}=s^*_{lm}$ and analogous relations for t_{lm}, s^A_{lm}, t^A_{lm}, and φ_{lm}. The definition (31) implies the following orthogonality relation for the $Y_{lm}(\theta,\phi)$:

$$\int_0^{2\pi} d\phi\int_0^{\pi} \sin\,\theta\, d\theta\, Y^*_{l'm'}(\theta,\phi)Y_{lm}(\theta,\phi)=\delta_{ll'}\delta_{mm'}. \tag{32}$$

A useful relation is

$$\Omega\, Y_{lm}=-\,l(l+1)Y_{lm}, \tag{33}$$

where the operator Ω is defined by

$$\Omega f=\frac{1}{\sin\,\theta}\frac{\partial}{\partial\,\theta}\left(\sin\,\theta\frac{\partial f}{\partial\,\theta}\right)+\frac{1}{\sin^2\theta}\frac{\partial^2 f}{\partial\,\phi^2}. \tag{34}$$

From Eqs. (28)–(30) we obtain, with the help of Eq. (33), the components of **B**,

$$B_r(r,\theta,\phi)=\sum_{l,m}\frac{l(l+1)}{r^2}s_{lm}(r)Y_{lm}(\theta,\phi),$$

$$B_\theta(r,\theta,\phi)=\sum_{l,m}\left(\frac{t_{lm}(r)}{r\,\sin\,\theta}\frac{\partial Y_{lm}(\theta,\phi)}{\partial\,\phi}+\frac{1}{r}\frac{ds_{lm}(r)}{dr}\frac{\partial Y_{lm}(\theta,\phi)}{\partial\,\theta}\right),$$

$$B_\phi(r,\theta,\phi)=\sum_{l,m}\left(-\frac{t_{lm}(r)}{r}\frac{\partial Y_{lm}(\theta,\phi)}{\partial\,\theta}+\frac{1}{r\,\sin\,\theta}\frac{ds_{lm}(r)}{dr}\frac{\partial Y_{lm}(\theta,\phi)}{\partial\,\phi}\right), \tag{35}$$

and equivalent expressions for the components of **A**, in which $s_{lm}(r)$ and $t_{lm}(r)$ are replaced by $s^A_{lm}(r)$ and $t^A_{lm}(r)$, respectively.

Finally, we recall the expression for the inverse distance between two points $\mathbf{r}$ and $\mathbf{r}'$,

$$\frac{1}{|\mathbf{r}-\mathbf{r}'|}=4\pi\sum_{l=0}^{\infty}\sum_{m=-l}^{l}\frac{1}{2l+1}\frac{r_<^l}{r_>^{l+1}}Y^*_{lm}(\theta',\phi')Y_{lm}(\theta,\phi), \tag{36}$$

where $r_>$ denotes the larger of the values r and r', and $r_<$ the smaller one.

Equipped with these preliminaries, the two coupled integral equations for the functions $s_{lm}(r)$ and $t_{lm}(r)$ can be derived. This is done in Appendix A, both as a dimensional reduction of the basic integral equation system and from the radial differential equation system by using the Green's function method. Here we give only the final form of the integral equation system for $s_{lm}(r)$ and $t_{lm}(r)$:

$$s_{lm}(r)=\frac{\mu_0\sigma}{2l+1}\left[\int_0^r\frac{r'^{l+1}}{r^l}\alpha(r')t_{lm}(r')dr'+\int_r^R\frac{r^{l+1}}{r'^l}\alpha(r')t_{lm}(r')dr'-\lambda\int_0^r\frac{r'^{l+1}}{r^l}s_{lm}(r')dr'-\lambda\int_r^R\frac{r^{l+1}}{r'^l}s_{lm}(r')dr'\right] \tag{37}$$

and

$$t_{lm}(r)=\mu_0\sigma\left[\alpha(r)s_{lm}(r)-\frac{l+1}{2l+1}\int_0^r\frac{d\alpha(r')}{dr'}s_{lm}(r')\frac{r'^l}{r^l}dr'+\frac{l}{2l+1}\int_r^R\frac{d\alpha(r')}{dr'}s_{lm}(r')\frac{r^{l+1}}{r'^{l+1}}dr'+\frac{l+1}{2l+1}\frac{r^{l+1}}{R^{2l+1}}\int_0^R r'^l\frac{d\alpha(r')}{dr'}s_{lm}(r')dr'+\frac{\lambda}{2l+1}\frac{r^{l+1}}{R^{2l+1}}\int_0^R r'^{l+1}t_{lm}(r')dr'-\frac{\lambda}{2l+1}\int_0^r\frac{r'^{l+1}}{r^l}t_{lm}(r')dr'-\frac{\lambda}{2l+1}\int_r^R\frac{r^{l+1}}{r'^l}t_{lm}(r')dr'-\frac{r^{l+1}}{R^{l+1}}\alpha(R)s_{lm}(R)\right]. \tag{38}$$

Notwithstanding the fact that the differential and integral equation approaches are equivalent in a general sense, it might be instructive to show this equivalence for our special problem. Differentiating Eqs. (37) and (38) two times with respect to the radial component the following relations can be obtained:

$$\lambda s_{lm}=\frac{1}{\mu_0\sigma}\left[\frac{d^2s_{lm}}{dr^2}-\frac{l(l+1)}{r^2}s_{lm}\right]+\alpha(r)t_{lm}, \tag{39}$$

$$\lambda t_{lm}=\frac{1}{\mu_0\sigma}\left[\frac{d^2t_{lm}}{dr^2}-\frac{l(l+1)}{r^2}t_{lm}\right]-\frac{d}{dr}\left(\alpha(r)\frac{ds_{lm}}{dr}\right)+\frac{l(l+1)}{r^2}\alpha(r)s_{lm}, \tag{40}$$

$$t_{lm}(R)=\left.R\frac{ds_{lm}(r)}{dr}\right|_{r=R}+ls_{lm}(R)=0. \tag{41}$$

As expected, these are the differential equations for the considered problem of radially varying α for the time-dependent case [31,34].

B. Numerics

1. Discretization

In the previous section and in Appendix A, we have derived the radial integral equations (37) and (38) governing the time-dependent dynamo problem. In this subsection, we develop a numerical method to solve this integral equation system.

Let us introduce the following definitions:

$$x = r/R, \quad C\alpha(x) = R^2\mu_0\sigma\alpha(r), \quad \tilde{\lambda}_l = R^2\mu_0\sigma\lambda_l, \quad (42)$$

where C is the magnitude of the function $R^2\mu_0\sigma\alpha$. In addition, we introduce the notations

$$G_s(x,x_0) = \begin{cases} -\dfrac{1}{2l+1}x_0^{-l}x^{l+1}, & x \leqslant x_0, \\ -\dfrac{1}{2l+1}x_0^{l+1}x^{-l}, & x \geqslant x_0, \end{cases} \quad (43)$$

$$G_t(x,x_0) = \begin{cases} \dfrac{1}{2l+1}(x_0^{l+1} - x_0^{-l})x^{l+1}, & x \leqslant x_0, \\ \dfrac{1}{2l+1}(x^{l+1} - x^{-l})x_0^{l+1}, & x \geqslant x_0, \end{cases} \quad (44)$$

$$\overline{G}_t(x,x_0) = \begin{cases} \dfrac{l+1}{2l+1}x_0^l x^{l+1} + \dfrac{l}{2l+1}x_0^{-l-1}x^{l+1}, & x \leqslant x_0, \\ \dfrac{l+1}{2l+1}x_0^l x^{l+1} + \dfrac{l}{2l+1}x^{-l}x_0^l, & x \geqslant x_0. \end{cases} \quad (45)$$

Then, Eqs. (37) and (38) obtain the form

$$s_{lm}(x) = -C\int_0^1 G_s(x,x_0)\alpha(x_0)t_{lm}(x_0)dx_0 + \tilde{\lambda}_l\int_0^1 G_s(x,x_0)s_{lm}(x_0)dx_0, \quad (46)$$

$$t_{lm}(x) = C\alpha(x)s_{lm}(x) - Cx^{l+1}\alpha(1.0)s_{lm}(1.0) + C\int_0^1 \frac{d\alpha(x_0)}{dx_0}s_{lm}(x_0)\overline{G}_t(x,x_0)dx_0 + \tilde{\lambda}_l\int_0^1 G_t(x,x_0)t_{lm}(x_0)dx_0 - C\int_0^x x^{-l}x_0^l\frac{d\alpha(x_0)}{dx_0}s_{lm}(x_0)dx_0. \quad (47)$$

Choosing N equidistant grid points $x_i = i\Delta x$ with $\Delta x = 1/N$ and approximating the integrals by the extended trapezoidal rule according to

$$\int_0^1 f(x)dx \approx \sum_{i=1}^{N}\frac{1}{2}[f(x_{i-1}) + f(x_i)]\Delta x, \quad (48)$$

we obtain

$$\tilde{\lambda}_l\sum_{j=1}^{N} s_{lm}(x_j)G_s(x_i,x_j)\Delta x c_j = s_{lm}(x_i) + C\sum_{j=1}^{N-1}\alpha(x_j)t_{lm}(x_j)G_s(x_i,x_j)c_j\Delta x, \quad (49)$$

$$\tilde{\lambda}_l\sum_{j=1}^{N-1} G_t(x_i,x_j)t_{lm}(x_j)\Delta x c_j = t_{lm}(x_i) - C\alpha(x_i)s_{lm}(x_i) + Cx_i^{l+1}\alpha(1.0)s_{lm}(1.0) - C\sum_{j=1}^{N}\frac{d\alpha(x_j)}{dx}s_{lm}(x_j)\overline{G}_t(x_i,x_j)\Delta x c_j + C\sum_{j=1}^{i} x_i^{-l}x_j^l\frac{d\alpha(x_j)}{dx}s_{lm}(x_j)\Delta x c_j, \quad (50)$$

where $c_N = 0.5$ and $c_i = 1.0$ for $i = 1,2,\ldots,N-1$. Equations (49) and (50) can be written in the matrix form

$$\tilde{\lambda}_l\mathbf{V}\mathbf{X} = \mathbf{W}\mathbf{X}, \quad (51)$$

with

$$\mathbf{X} = (s_{lm}(x_1), s_{lm}(x_2), \ldots, s_{lm}(x_N), t_{lm}(x_1), t_{lm}(x_2), \ldots, t_{lm}(x_{N-1}))^T,$$

$$V_{i,j} = G_s(x_i,x_j)\Delta x c_j \quad (i,j = 1,2,\ldots,N),$$

$$V_{i+N,j} = 0 \quad (i = 1,2,\ldots,N-1, j = 1,2,\ldots,N),$$

$$V_{i,j+N} = 0 \quad (i = 1,2,\ldots,N, j = 1,2,\ldots,N-1),$$

$$V_{i+N,j+N} = G_t(x_i,x_j)c_j\Delta x \quad (i = 1,2,\ldots,N-1, j = 1,2,\ldots,N-1),$$

$$W_{i,j} = \delta(i,j) \quad (i,j = 1,2,\ldots,N),$$

$$W_{i,j+N} = G_s(x_i,x_j)\Delta x c_j\alpha(x_j) \quad (i = 1,2,\ldots,N, j = 1,2,\ldots,N-1),$$

$$W_{i+N,j+N} = \delta(i,j) \quad (i,j = 1,2,\ldots,N-1),$$

$$W_{i+N,j} = -C\frac{d\alpha(x_j)}{dx}\overline{G}_t(x_i,x_j)\Delta x c_j - C\alpha(x_i)\delta(i,j) + Cx_i^{l+1}\alpha(1.0)\delta(j,N) + Cx_i^{-l}x_j^l\frac{d\alpha(x_j)}{dx}\Delta x c_j H(i-j) \quad (i = 1,2,\ldots,N-1, j = 1,2,\ldots,N), \quad (52)$$

where the functions $\delta(i,j)$ and $H(i-j)$ are defined as

$$\delta(i,j) = \begin{cases} 0, & i \neq j, \\ 1, & i = j, \end{cases}$$

and

TABLE I. Comparison of the calculated growth rates and the analytic ones for the free decay case $\alpha(x)=0$. The degree of the spherical harmonics is $l=1$. $n=1,\ldots,4$ correspond to modes with increasing radial wave number n. The last row shows the analytic results. The other rows express the numerical results obtained by the integral equation approach for different grid numbers N.

N	$n=1$	$n=2$	$n=3$	$n=4$
8	−9.79494	−37.71179	−79.61435	−129.36969
16	−9.85079	−39.02608	−86.41265	−150.20904
32	−9.86485	−39.36475	−88.21583	−155.94894
64	−9.86844	−39.44979	−88.67356	−157.42004
128	−9.86933	−39.47085	−88.78596	−157.78870
Analytic	−9.86960	−39.47842	−88.82644	−157.91367

$$H(i-j)=\begin{cases}1, & i\geqslant j,\\ 0, & i<j.\end{cases}$$

Note that Eq. (51) is a linear generalized eigenvalue problem. By multiplying both sides of Eq. (51) by the inverse of the matrix $\mathbf{V}$, we can convert it to the following standard eigenvalue problem:

$$\mathbf{V}^{-1}\mathbf{W}\mathbf{X}=\tilde{\lambda}_l\mathbf{X}. \tag{53}$$

This eigenvalue problem can be solved by standard numerical routines. First, the matrix $\mathbf{V}^{-1}\mathbf{W}$ is reduced to the Hessenberg form; then, the QR algorithm can be employed to obtain the eigenvalue $\tilde{\lambda}_l$.

2. Numerical results

In this subsection, we illustrate the numerical performance of the integral equation approach formulated in this paper by a few examples for the functions $\alpha(x)$.

Let us start with the case $\alpha(x)=0$, which corresponds to a pure field decay within a conducting sphere. For this case, the eigenvalues $\tilde{\lambda}_l$ are known from quasianalytic calculations [1]. In Table I (for $l=1$) and Table II (for $l=2$) we have listed the numerical results of the integral equation solver for the eigenmodes with increasing radial wave numbers $n=1,\ldots,4$, together with the analytical results. From these tables it becomes obvious that even for a few grid numbers robust results can be obtained. In Figs. 1 and 2 we have plotted the relative errors of the results in dependence on the used number of grid points N. As is typical for integral equations of that kind [20], the relative error decreases like N^{-2}.

TABLE II. Same as Table I, but for $l=2$.

N	$n=1$	$n=2$	$n=3$	$n=4$
8	−19.87668	−55.87647	−103.28617	−155.45810
16	−20.11100	−58.68925	−114.71107	−186.07856
32	−20.17073	−59.42935	−117.83333	−194.82947
64	−20.18561	−59.61664	−118.63189	−197.09552
128	−20.18911	−59.66311	−118.83366	−197.66728
Analytic	−20.19073	−59.67951	−118.89986	−197.85780

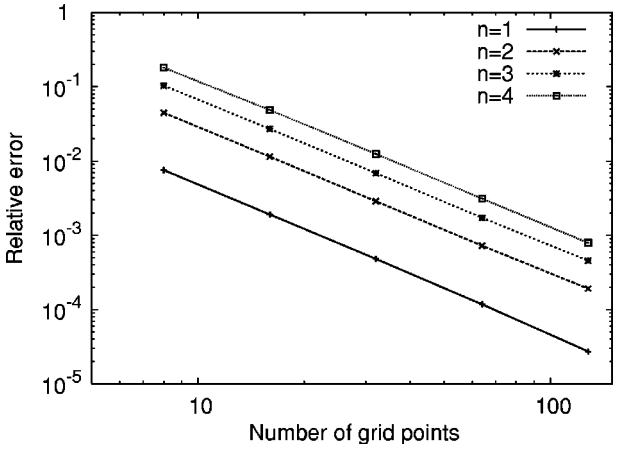

FIG. 1. Relative error of the numerically determined eigenvalues for the free decay case, $C=0$, $l=1$, $n=1,\ldots,4$. The convergence behaves like N^{-2}.

Another quasianalytic result exists for the steady case [1]: for $l=1$ and $C=4.493\,409\,5$ or $l=2$ and $C=5.763\,459\,3$ we know that the first eigenvalues have to be zero. Table III shows the results of the integral equation solver, again for $l=1$ and $l=2$, but only for $n=1$. The convergence of the results, which is again $\sim N^{-2}$, is depicted in Fig. 3.

Now, we turn to a more complicated case. It corresponds to the profile $\alpha(x)=C(-21.46+426.41x^2-806.73x^3+392.28x^4)$. The choice of this somewhat strange function is motivated by the fact that it is an example of a proper oscillatory α^2 dynamo [31]. In Fig. 4 we show the results of the integral equation solver for the case $l=1$ and $n=1,\ldots,7$. We see that the spectral dependence on C (Fig. 4) is very complex, with merging and splitting points of neighboring branches at which nonoscillatory solutions turn into oscillatory solutions and vice versa. The computation was done with a grid number of $N=128$, and the result is basically identical with that of a sophisticated differential equation solver [31]. Hence, Fig. 4 might serve as a striking example that the integral equation approach works satisfactorily also in case that complex eigenvalues appear.

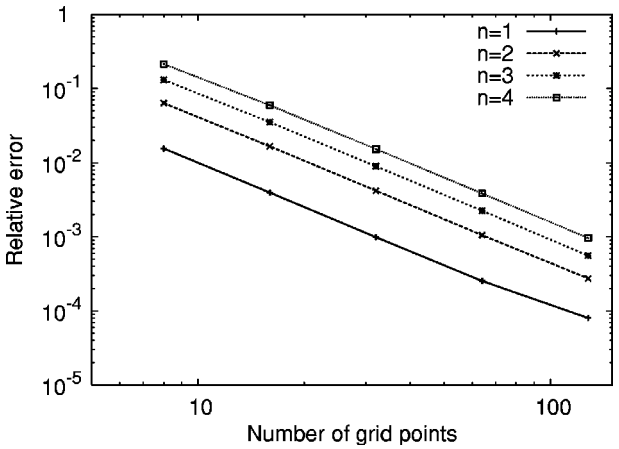

FIG. 2. Same as Fig. 1, but for $l=2$.

TABLE III. Convergence of the first eigenvalue ($n=1$) to zero in the cases: $C=4.493\,409\,5, l=1$ and $C=5.763\,459\,3, l=2$. The normalization of the errors is done with the growth rates at $C=0$, which are $\lambda_1(C=0)=-9.8696$ and $\lambda_2(C=0)=-20.1907$.

l	$N=8$	$N=16$	$N=32$	$N=64$	$N=128$
1	0.19836	0.04971	0.01249	0.00355	0.00052
2	0.58527	0.14903	0.03740	0.01010	0.00072

IV. GENERAL VELOCITY FIELDS IN SPHERICAL GEOMETRY

A. Radial integral equation system

In this section the Green's function method from Appendix A 2 is applied to convert the induction equation for general velocity fields in a unit sphere to the integral equation system. In dimensionless form, Eq. (1) can be rewritten as follows:

$$\frac{\partial \mathbf{B}}{\partial t} = R_m \boldsymbol{\nabla} \times (\mathbf{u} \times \mathbf{B}) + \boldsymbol{\nabla}^2 \mathbf{B}, \tag{54}$$

where R_m is the magnetic Reynolds number. **u** and **B** may be expanded into the following series [35]:

$$\mathbf{u} = \sum_{\alpha} (\mathbf{t}_\alpha + \mathbf{s}_\alpha), \tag{55}$$

$$\mathbf{B} = \sum_{\beta} (\mathbf{T}_\beta + \mathbf{S}_\beta), \tag{56}$$

where

$$\mathbf{t}_\alpha = \boldsymbol{\nabla} \times [\mathbf{e}_r t_\alpha(r,t) Y_\alpha(\theta,\varphi)], \tag{57}$$

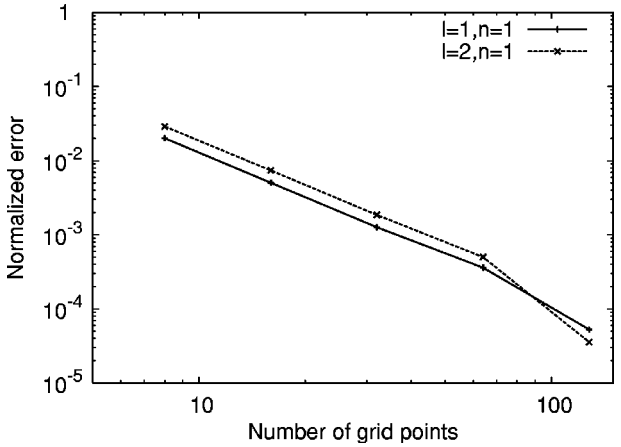

FIG. 3. Convergence of the first eigenvalue ($n=1$) to zero in the cases: $C=4.493\,409\,5, l=1$ and $C=5.763\,459\,3, l=2$. The normalization of the error is done with respect to the growth rates at $C=0$ which are $\lambda_1=-9.8696$ and $\lambda_1=-20.1907$.

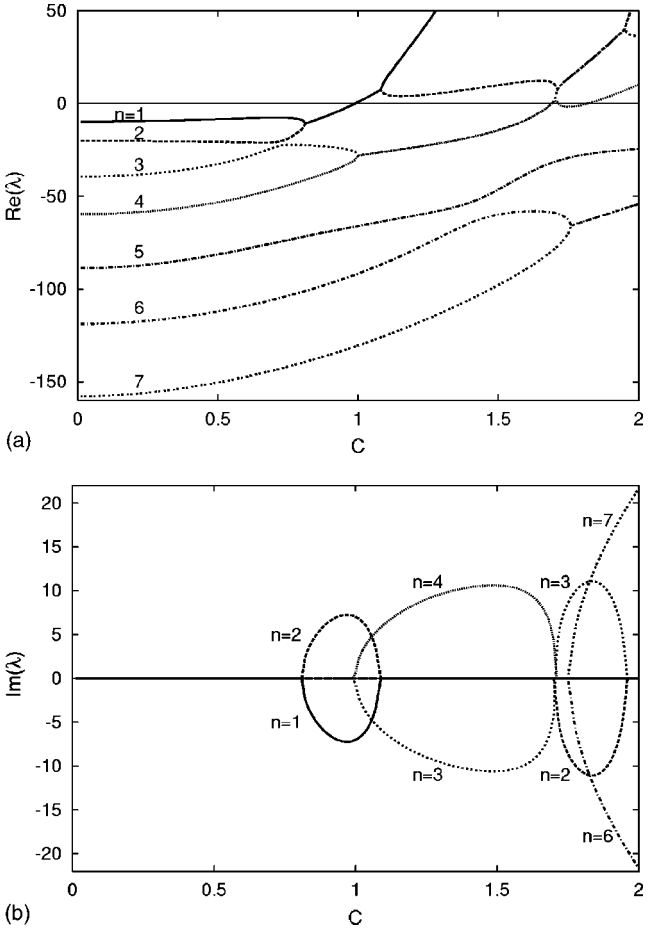

FIG. 4. Special case $\alpha(x)=C(-21.46+426.41x^2-806.73x^3+392.28x^4)$. Growth rates and frequencies for the eigenfunctions with $(l=1, n=1,\ldots,7)$. The number of grid points was $N=128$. Note the merging and splitting points of the spectrum, indicating transitions from nonoscillatory to oscillatory modes and vice versa.

$$\mathbf{s}_\alpha = \boldsymbol{\nabla} \times \boldsymbol{\nabla} \times [\mathbf{e}_r s_\alpha(r,t) Y_\alpha(\theta,\varphi)], \tag{58}$$

etc. From here on, Y_α denote the $(2\alpha+1)$ surface harmonics $P_{\alpha m_\alpha}(\theta)\sin(m_\alpha\varphi)$, $P_{\alpha m_\alpha}(\theta)\cos(m_\alpha\varphi)$ $(m_\alpha=0,\ldots,\alpha)$, where $P_{\alpha m_\alpha}$ is a Legendre function with Neumann normalization and $P_{\alpha 0}$ the Legendre polynomial. Similarly s_α is an abbreviation for $s_\alpha^{m_\alpha}$, etc. The summations in Eqs. (55) and (56) are over cosine and sine contributions, $\alpha=1,2,3,\ldots;m_\alpha=0,\ldots,\alpha$; and similarly for β, m_β. Substituting Eqs. (55) and (56) into Eq. (54), Bullard and Gellman [35] derived the spectral form of Eq. (54) as

$$\frac{\partial^2 S_\gamma}{\partial r^2} - \frac{\partial S_\gamma}{\partial t} - \frac{\gamma(\gamma+1)}{r^2} S_\gamma = \frac{R_m}{r^2} \sum_{\alpha,\beta} [(t_\alpha S_\beta S_\gamma) + (s_\alpha T_\beta S_\gamma) + (s_\alpha S_\beta S_\gamma)], \tag{59}$$

$$\frac{\partial^2 T_\gamma}{\partial r^2} - \frac{\partial T_\gamma}{\partial t} - \frac{\gamma(\gamma+1)}{r^2} T_\gamma = \frac{R_m}{r^2} \sum_{\alpha,\beta} [(t_\alpha T_\beta T_\gamma) + (t_\alpha S_\beta T_\gamma) + (s_\alpha T_\beta T_\gamma) + (s_\alpha S_\beta T_\gamma)], \quad (60)$$

where

$$(t_\alpha S_\beta S_\gamma) = c_1 t_\alpha S_\beta,$$

$$(s_\alpha T_\beta S_\gamma) = c_2 s_\alpha T_\beta,$$

$$(s_\alpha S_\beta S_\gamma) = c_3 s_\alpha \frac{\partial S_\beta}{\partial r} + c_4 \frac{\partial s_\alpha}{\partial r} S_\beta,$$

$$(t_\alpha T_\beta T_\gamma) = c_5 t_\alpha T_\beta,$$

$$(t_\alpha S_\beta T_\gamma) = c_6 t_\alpha \frac{\partial S_\beta}{\partial r} + c_7 \left(\frac{\partial t_\alpha}{\partial r} - \frac{2t_\alpha}{r} \right) S_\beta,$$

$$(s_\alpha T_\beta T_\gamma) = c_8 s_\alpha \frac{\partial T_\beta}{\partial r} + c_8 \left(\frac{\partial s_\alpha}{\partial r} - \frac{2s_\alpha}{r} \right) T_\beta + c_9 \frac{\partial s_\alpha}{\partial r} T_\beta,$$

$$(s_\alpha S_\beta T_\gamma) = c_{10} s_\alpha \frac{\partial^2 S_\beta}{\partial r^2} + c_{11} \frac{\partial s_\alpha}{\partial r} \frac{\partial S_\beta}{\partial r} + c_{12} \frac{s_\alpha}{r} \frac{\partial S_\beta}{\partial r} + c_{13} \left(\frac{\partial^2 s_\alpha}{\partial r^2} - \frac{2}{r} \frac{\partial s_\alpha}{\partial r} \right) S_\beta. \quad (61)$$

The constants c_i in Eq. (61) are defined in the Appendix B.

By the same Green's functions method as in Appendix A, and using the definitions for $G_s(r,r_0)$, $G_t(r,r_0)$ there, the differential equations system (59) and (60) can be converted to the following integral equations system:

$$S_\gamma(r) = \sum_{\alpha\beta} R_m \int_0^1 \frac{G_s(r,r_0)}{r_0^2} \left[c_1 t_\alpha(r_0) S_\beta(r_0) + c_2 s_\alpha(r_0) T_\beta(r_0) + c_3 s_\alpha(r_0) \frac{dS_\beta(r_0)}{dr_0} + c_4 \frac{ds_\alpha(r_0)}{dr_0} S_\beta(r_0) \right] dr_0 + \lambda \int_0^1 G_s(r,r_0) S_\gamma(r_0) dr_0, \quad (62)$$

$$T_\gamma(r) = \sum_{\alpha\beta} R_m \int_0^1 \frac{G_t(r,r_0)}{r_0^2} \left[c_5 t_\alpha(r_0) T_\beta(r_0) + c_6 t_\alpha(r_0) \frac{dS_\beta(r_0)}{dr_0} + c_7 \left(\frac{dt_\alpha(r_0)}{dr_0} - \frac{2t_\alpha(r_0)}{r_0} \right) S_\beta(r_0) + c_8 s_\alpha(r_0) \frac{dT_\beta(r_0)}{dr_0} + c_8 \left(\frac{ds_\alpha(r_0)}{dr_0} - \frac{2}{r_0} s_\alpha(r_0) \right) T_\beta(r_0) + c_9 \frac{ds_\alpha(r_0)}{dr_0} T_\beta(r_0) + c_{10} s_\alpha(r_0) \frac{d^2 S_\beta(r_0)}{dr_0^2} + c_{11} \frac{ds_\alpha(r_0)}{dr_0} \frac{dS_\beta(r_0)}{dr_0} + c_{12} \frac{s_\alpha(r_0)}{r_0} \frac{dS_\beta(r_0)}{dr_0} + c_{13} \left(\frac{d^2 s_\alpha(r_0)}{dr_0^2} - \frac{2}{r_0} \frac{ds_\alpha(r_0)}{dr_0} \right) S_\beta(r_0) \right] dr_0 + \lambda \int_0^1 G_t(r,r_0) T_\gamma(r_0) dr_0. \quad (63)$$

Strictly speaking, this is an integro-differential equation system which could be used for numerical analysis. If one would insist on having a pure integral equation system, one could employ integration by parts in order to obtain

$$S_\gamma(r) = \sum_{\alpha\beta} R_m \left[\int_0^1 G_s(r,r_0) F_1(r_0) S_\beta(r_0) dr_0 + \int_0^1 G_s(r,r_0) F_2(r_0) T_\beta(r_0) dr_0 + \int_0^1 \frac{\partial G_s(r,r_0)}{\partial r_0} F_3(r_0) S_\beta(r_0) dr_0 - \frac{c_3}{2\gamma+1} r^{\gamma+1} s_\alpha(1.0) S_\beta(1.0) \right] + \lambda \int_0^1 G_s(r,r_0) S_\gamma(r_0) dr_0, \quad (64)$$

$$T_\gamma(r) = \sum_{\alpha\beta} R_m \left[\int_0^1 G_t(r,r_0) F_4(r_0) T_\beta(r_0) dr_0 + \int_0^1 G_t(r,r_0) F_5(r_0) S_\beta(r_0) dr_0 + \int_0^1 \frac{\partial G_t(r,r_0)}{\partial r_0} F_6(r_0) S_\beta(r_0) dr_0 + \int_0^1 \frac{\partial G_t(r,r_0)}{\partial r_0} F_7(r_0) T_\beta(r_0) dr_0 - c_{10} r^{\gamma+1} s_\alpha(1.0) S_\beta(1.0) + \frac{c_{10}}{r^2} S_\alpha(r) S_\beta(r) \right] + \lambda \int_0^1 G_t(r,r_0) T_\gamma(r_0) dr_0, \quad (65)$$

with

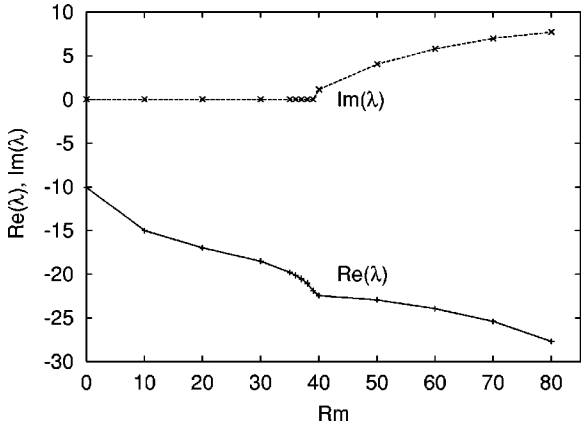

FIG. 5. Real and imaginary parts of the first eigenvalue for the Bullard-Gellman dynamo model in dependence on the magnetic Reynolds number. The truncation degree is $L=9$, and the number of radial grid points is $N=75$.

$$F_1 = c_1\frac{t_\alpha}{r_0^2} - c_3\frac{d}{dr_0}\left(\frac{s_\alpha}{r_0^2}\right) + c_4\frac{1}{r_0^2}\frac{ds_\alpha}{dr_0},$$

$$F_2 = c_2\frac{s_\alpha}{r_0^2},$$

$$F_3 = -c_3\frac{s_\alpha}{r_0^2},$$

$$F_4 = c_5\frac{t_\alpha}{r_0^2} - c_8\frac{d}{dr_0}\left(\frac{s_\alpha}{r_0^2}\right) + c_8\frac{1}{r_0^2}\left(\frac{ds_\alpha}{dr_0} - \frac{2}{r_0}s_\alpha\right) + c_9\frac{1}{r_0^2}\frac{ds_\alpha}{dr_0},$$

$$F_5 = -c_6\frac{d}{dr_0}\left(\frac{t_\alpha}{r_0^2}\right) + c_7\frac{1}{r_0^2}\left(\frac{dt_\alpha}{dr_0} - \frac{2}{r_0}t_\alpha\right) + c_{10}\gamma(\gamma+1)\frac{s_\alpha}{r_0^4} + c_{10}\frac{d^2}{dr_0^2}\left(\frac{s_\alpha}{r_0^2}\right) - c_{11}\frac{d}{dr_0}\left(\frac{1}{r_0^2}\frac{ds_\alpha}{dr_0}\right) - c_{12}\frac{d}{dr_0}\left(\frac{s_\alpha}{r_0^3}\right) + c_{13}\frac{1}{r_0^2}\left(\frac{d^2s_\alpha}{dr_0^2} - \frac{2}{r_0}\frac{ds_\alpha}{dr_0}\right),$$

$$F_6 = -c_6\frac{t_\alpha}{r_0^2} + 2c_{10}\frac{d}{dr_0}\left(\frac{s_\alpha}{r_0^2}\right) - c_{11}\frac{1}{r_0^2}\frac{ds_\alpha}{dr_0} - c_{12}\frac{s_\alpha}{r_0^3},$$

$$F_7 = -c_8\frac{s_\alpha}{r_0^2}.$$

The discretization of this integral equation system is done along the lines described in Sec. III B 1.

B. Numerical example: The Bullard-Gellman model

In the following, we will test the suitability of the integral equation approach to the simulation of large-scale velocity fields for a particular dynamo model. In 1954, Bullard and Gellman [35] studied the flow structure

$$\mathbf{u} = \mathbf{s}_2^{2c} + 5\mathbf{t}_1^0, \tag{66}$$

where

$$s_2^{2c}(r) = r^3(1-r)^2, \tag{67}$$

$$t_1^0(r) = r^2(1-r), \tag{68}$$

claiming that this flow acts indeed as a dynamo. Later, using higher spatial resolution, Gibson, Roberts, and Scott, [36] and Dudley and James [37] falsified this result, showing that there is no dynamo up to a magnetic Reynolds number of 80.

Here we treat the Bullard-Gellman model within the framework of the integral equation approach.

In Fig. 5 we plot the real and imaginary parts of the first eigenvalue of the D1 solution (in the terminology of Dudley and James) for the Bullard-Gellman dynamo model in dependence on the magnetic Reynolds number. The truncation degree is $L=9$, and the number of radial grid points is $N=75$. This is essentially the same curve as published in [37] where a truncation degree $L=12$ and a number of grid points of $N=100$ had been used, however.

In Table IV we have compiled some results concerning the convergence of our method and the method of Dudley and James. For $Rm=50$ (where no data are available from Dudley and James) we see a reasonable convergence of the real part but a slow convergence of the imaginary part. The latter might be due to the fact that we are not far from the transition point to oscillatory behavior where the imaginary part is sensible to changes in the grid number. For $Rm=80$ we have to concede that the convergence in our case is slower than in the differential equation method of Dudley and James.

A similar conclusion can be drawn from the treatment of other models (Lilley model, modified Lilley model). Although our method yields essentially the same results as the differential equation approach, it seems worth to look for refined numerical methods to solve the integral eigenvalue equation.

TABLE IV. Convergence of the integral equation approach (IEA) and the Dudley and James method (DJ). We show the dependence of λ on the radial grid number N for $Rm=50$ and $Rm=80$ using a truncation degree $L=9$. The interpolation in the IEA case is done with a fit of the date to a function $a+bN^{-2}$. Dudley and James had used Richardson extrapolation based on the values for $N=75,100,125$.

	$N=50$	$N=75$	$N=100$	$N=125$	Extrapolation
IEA $Rm=50$	$-23.50+4.97i$	$-22.97+4.03i$	$-22.76+3.66i$	$-22.63+3.34i$	
IEA $Rm=80$	$-29.35+9.46i$	$-27.70+7.72i$	$-26.95+6.98i$	$-26.51+6.57i$	$-26.10+6.26i$
DJ $Rm=80$		$-26.32+6.01i$	$-26.33+6.04i$	$-26.33+6.05i$	$-26.34+6.06i$

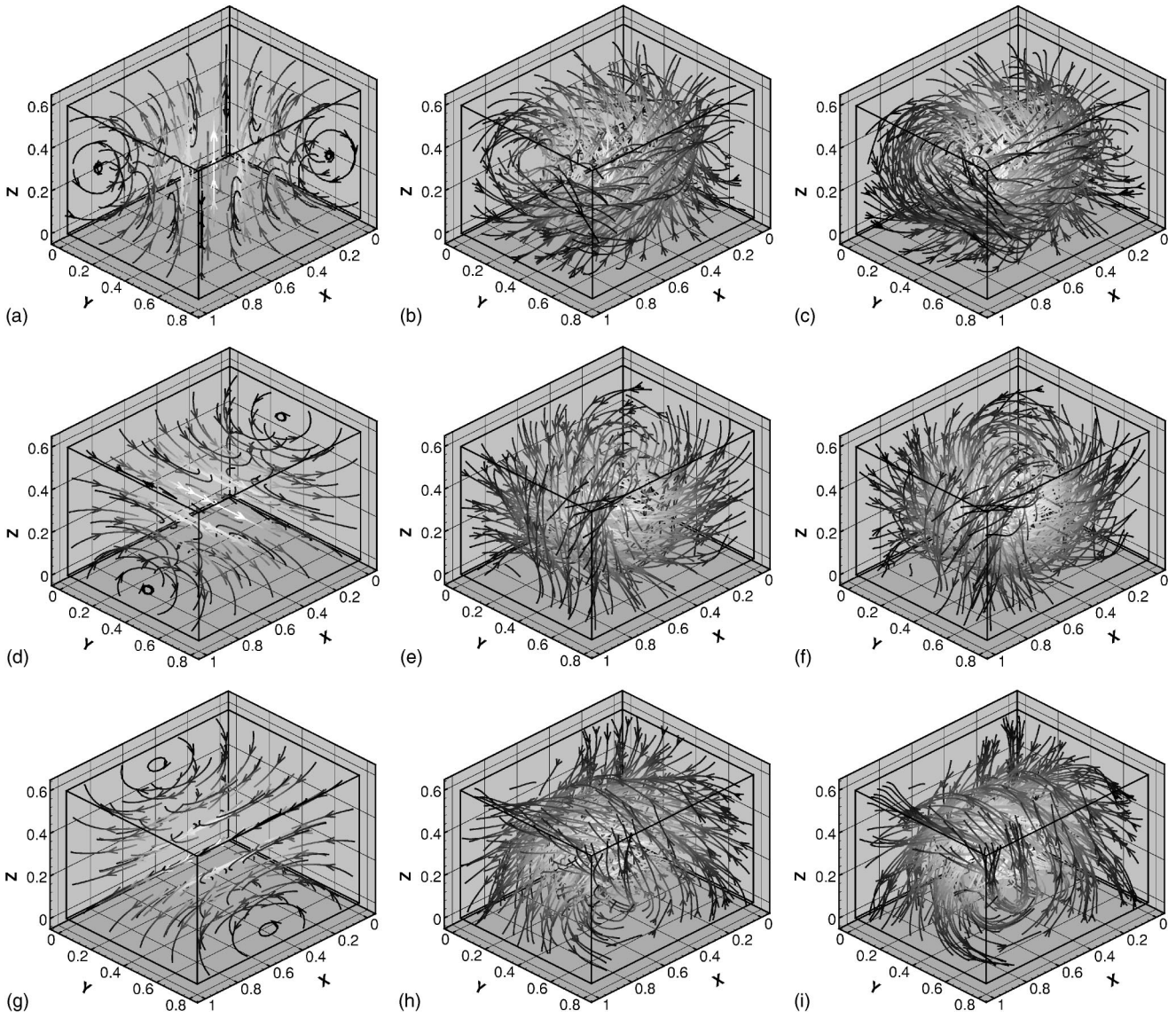

FIG. 6. Magnetic eigenfields belonging to the three lowest eigenvalues (ordered from top to bottom) of the α^2 dynamo in a "matchbox" with a sidelengths ratio of 1:0.8:0.6. The corresponding values of C' are 0, 1.943, and 4.593 (from left to right). The latter value $C'=4.593$ is the critical value for the first eigenmode. The gray scale of the field lines indicates the field strength.

V. GENERAL NUMERICAL SCHEME AND ITS APPLICATION TO RECTANGULAR DYNAMOS

In order to demonstrate the applicability of the integral equation approach, we consider here the case of an arbitrary geometry. First, we delineate the general numerical scheme; then, we will apply it to dynamos in rectangular geometry. Needless to say, this geometry is only of academic interest, but it illustrates nicely the main advantage of the integral equation approach.

A. General numerical scheme

Here we delineate the general framework for the numerical solution of the coupled equations (20), (24), and (27). Let us assume certain spatial discretizations of the magnetic field and the vector potential in the volume of the dynamo and of the electric potential at the boundary. Then, Eq. (20) may be rewritten in the form

$$B_i = L_{ik}B_k + \lambda P_{ij}A_j + N_{il}\varphi_l, \tag{69}$$

where B_i and A_j denote the degrees of freedom of the magnetic field and the vector potential in the volume of the dynamo, while φ_l and A_n denote the degrees of freedom of the electric potential at the boundary. Here and in the following we use Einstein's summation convention, and we reserve the indices i,j,k for magnetic field and vector potential degrees of freedom in the volume of the fluid, whereas the indices l,m,n are reserved for the electric potential degrees of freedom at the boundary of the fluid.

For any given dynamo source, any shape of the dynamo domain, and any concrete form of the discretization, the matrices **L**, **N**, and **P** in Eq. (69) can easily be derived from Eq. (20). It is worthwhile noting that only **L** depends on the

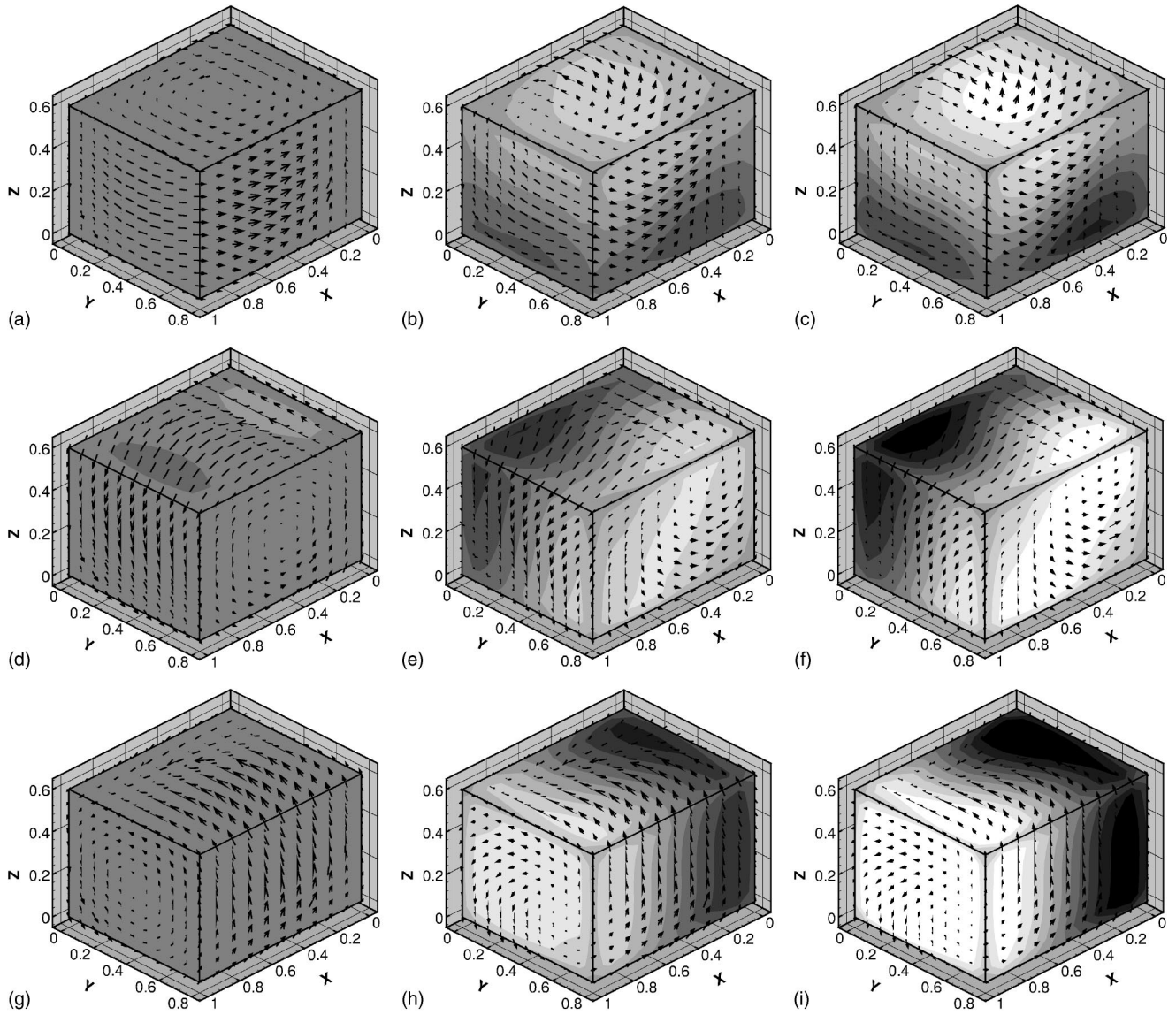

FIG. 7. Electric potential and magnetic vector potential at the box boundary belonging to the three lowest eigenvalues (ordered from top to bottom) of the α^2 dynamo in a box with sidelengths ratio 1:0.8:0.6. The corresponding values of C': 0, 1.943, and 4.593 (from left to right).

dynamo source (**u** or α), whereas **N** and **P** depend only on the geometry of the dynamo domain and the discretization details.

Similarly, the discretization of the boundary integral equation (24) (for the case that **r** is on the surface S) leads to

$$0.5\ \varphi_l + E_{lm}\varphi_m = H_{lk}B_k + \lambda D_{lj}A_j \tag{70}$$

or

$$G_{lm}\varphi_m = H_{lk}B_k + \lambda D_{lj}A_j, \tag{71}$$

where $G_{lm}=0.5\ \delta_{lm}+E_{lm}$. Again one should note that only **H** depends on the dynamo source, whereas **G** and **D** depend only on the geometry of the dynamo domain and the discretization details. The discretization of Eq. (27) gives

$$A_j = Q_{jk}B_k, \tag{72}$$

with **Q** depending solely on the geometry.

Substituting Eq. (72) into Eq. (71) yields

$$\varphi_m = (G^{-1})_{ml}H_{lk}B_k + \lambda(G^{-1})_{ml}D_{lj}Q_{jk}B_k. \tag{73}$$

However, for the inversion of the matrix **G** some care is needed. Basically, **G** is a singular matrix, reflecting the fact that the electric potential is determined only up to a constant. Accidently, it may happen that this singularity is weakened by inaccuracies due to the discretization. Nevertheless, one should be careful with the inversion. A convenient method to deal with the inversion is the application of the *deflation method* [38,39]. In the following, we will simply assume that the inverse of **G** has been found in an appropriate manner.

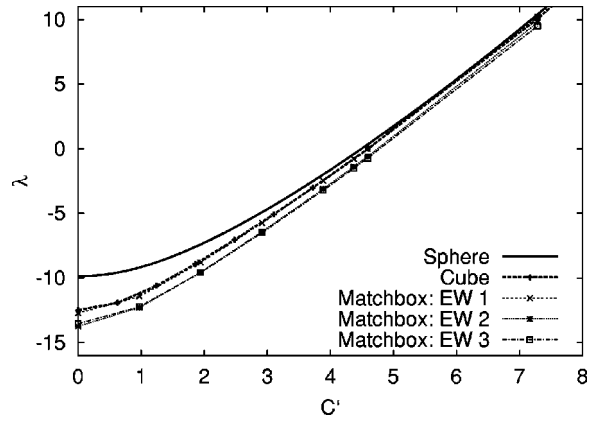

FIG. 8. Dependence of the eigenvalue λ on C' for the sphere, the cube, and the matchbox. For the sphere and the cube, the eigenvalue is threefold degenerated. For the matchbox, the degeneration is lifted. The length scale for the cube and the matchbox is chosen in such a way that their volume is equal to the volume of the unit sphere. Note the convergence of the leading eigenvalue for all three geometries with increasing C'.

After inserting Eqs. (72) and (73), Eq. (69) is transformed to

$$B_i = L_{ik}B_k + \lambda P_{ij}Q_{jk}B_k + N_{im}(G^{-1})_{ml}H_{lk}B_k + \lambda N_{il}(G^{-1})_{lm}D_{mj}Q_{jk}B_k. \quad (74)$$

Evidently, the electric potential at the boundary and the magnetic vector potential in the volume served only as auxiliary quantities in order to ensure the right boundary conditions. From the numerical viewpoint it is important to take notice of the following: for the accurate solution of the boundary integral equation (73) for a dynamo in a given domain it may be advisable to use a fine discretization of the boundary with a large number of grid points. Hence, the corresponding inversion of the matrix **G** might be numerically expensive. However, for a given geometry this inversion is needed only once. Finally, after carrying out the matrix multiplications $\mathbf{N}\cdot\mathbf{G}^{-1}\cdot\mathbf{H}$ and $\mathbf{N}\cdot\mathbf{G}^{-1}\cdot\mathbf{D}\cdot\mathbf{Q}$ in Eq. (74) one ends up with a matrix of the order (NB,NB) where NB denotes the total number of all magnetic field degrees of freedom.

Now, Eq. (74) can be rewritten in the following form:

$$[\delta_{ik} - L_{ik} - N_{im}(G^{-1})_{ml}H_{lk}]B_k = \lambda(P_{ij}Q_{jk} + N_{il}(G^{-1})_{lm}D_{mj}Q_{jk})B_k. \quad (75)$$

This is a generalized linear matrix eigenvalue problem in which only the magnetic field components remain. The numerical solution of the arising linear generalized eigenvalue equation (75) yields the eigenvalues λ, comprising as the real part the growth rate and as the imaginary part the frequency of the dynamo.

B. Application to rectangular dynamos

In the following we will apply the general numerical scheme to α^2 dynamos in rectangular geometry. Although this particular geometry is only of limited practical interest, it serves perfectly to illustrate the capabilities of our method.

More concretely, we will consider a cube and a "matchbox" with a side length's ratio of 1.0:0.8:0.6. In order to compare the results with the spherical pendant we choose a length scale such that we get the same volume as the unit sphere. That means, for the cube we use a side length of $\sqrt[3]{4\pi/3}=1.612$, and for the "matchbox" we use the longest side length as 2.0588. The domain is divided into 10^3 smaller rectangular boxes, with each face divided into 10^2 rectangles. For the steady case this problem has been treated in [20], and most of the details of the integral discretization can be found there. The additional terms related to the time-dependence are discretized in close analogy.

Using the code for the steady problem, in [20] we found the following critical values of $C' := \mu_0\sigma\alpha$ for the cubic case, the threefold degenerated critical value is $C'=4.599$; for the matchbox the three first critical values are $C'_1=4.593$, $C'_1=4.758$, and $C'_1=4.793$ (note that here C' refers to a box of the same volume as the unit sphere, whereas in [20] they refer to the cube of side length 2 and to a matchbox with the longest side equal to 2).

For the matchbox, we have visualized in Fig. 6 the magnetic field for the three first eigenvalues at the values $C'=0$, $C'=1.943$, and at the critical value $C'=4.593$. The corresponding electric potentials and vector potentials at the surface of the matchbox are shown in Fig. 7.

Looking at the free decay case $C'=0$, one can see a quite similar poloidal field structure as is well known in the spherical case. For increasing C' the magnetic field structure becomes more and more tangled and helical. The three eigenvectors correspond to three different positions of the dipolar axis. As expected, the magnetic field structure at the critical value $C'=4.593$ is the same as published in [20].

In Fig. 8 we plot now the dependence of the growth rate λ on C'. First we see that the free decay is faster than in the spherical case. However, for increasing α the growth rate of the leading eigenmode of both the cubic and the matchbox dynamo converges to that of its spherical pendant. This is a physically interesting result indicating that the boundary effects become less important with increasing α.

VI. REMARKS AND CONCLUSIONS

We have established the integral equation approach to time-dependent kinematic dynamos, with stationary dynamo sources, in arbitrary domains. This approach is based on the Biot-Savart law. The main advantage of the method is its suitability to handle dynamos in arbitrary domains. The necessity to solve the Laplace equation in the exterior of the dynamo domain is circumvented by the (implicit) solution of boundary integral equations for the electric potential and the magnetic vector potential.

It should be noted that we have worked out only one possible form of the integral equation approach which results in a linear eigenvalue problem. Another form could start from rewriting Eq. (18) into the form of a Helmholtz equation for the vector potential

$$\Delta\mathbf{A} - \mu_0\sigma\lambda\mathbf{A} = \mu_0\sigma(\mathbf{F} - \boldsymbol{\nabla}\varphi). \quad (76)$$

Then, the pendant to Eq. (20) would read

$$\mathbf{B}(\mathbf{r}) = \frac{\mu_0\sigma}{4\pi}\int_D \frac{\mathbf{F}(\mathbf{r}')\times(\mathbf{r}-\mathbf{r}')}{|\mathbf{r}-\mathbf{r}'|^3} \times\exp(k|\mathbf{r}-\mathbf{r}'|)(1-k|\mathbf{r}-\mathbf{r}'|)dV' - \frac{\mu_0\sigma}{4\pi}\int_S \varphi(\mathbf{s}')\mathbf{n}(\mathbf{s}')\frac{\mathbf{r}-\mathbf{s}'}{|\mathbf{r}-\mathbf{s}'|^3} \times\exp(k|\mathbf{r}-\mathbf{r}'|)(1-k|\mathbf{r}-\mathbf{r}'|)dS', \tag{77}$$

with

$$k = \sqrt{\lambda\mu_0\sigma}. \tag{78}$$

Without going into the details of such a formulation (we skip here the equations for the electric potential and the vector potential at the boundary), we see immediately that we end up with a nonlinear eigenvalue equation for the eigenvalue λ. It would be interesting to compare the numerical performance of such a formulation with the present one.

We plan to use our formulation for a number of dynamo problems, in particular problems which are connected with the design and optimization of new dynamo experiments and with the velocity reconstruction problem for the existing experiments.

ACKNOWLEDGMENT

Financial support from the German "Deutsche Forschungsgemeinschaft" in the framework of the Collaborative Research Center SFB 609 is gratefully acknowledged.

APPENDIX A: DERIVATION OF THE RADIAL INTEGRAL EQUATIONS FOR THE α^2-DYNAMO

1. Dimensional reduction of the integral equation system

a. Radial integral equation for $s_{lm}(r)$

Taking the scalar product of both sides of Eq. (20) with the unity vector $\mathbf{e}_r$ we obtain

$$\mathbf{B}(\mathbf{r})\cdot\mathbf{e}_r = \frac{\mu_0\sigma}{4\pi}\int_D \frac{[\alpha(r')\mathbf{B}(\mathbf{r}')-\lambda\mathbf{A}(\mathbf{r}')]\times(\mathbf{r}-\mathbf{r}')}{|\mathbf{r}-\mathbf{r}'|^3}\cdot\mathbf{e}_r\,dV' - \frac{\mu_0\sigma}{4\pi}\int_S \varphi(\mathbf{s}')\mathbf{n}(\mathbf{s}')\times\frac{\mathbf{r}-\mathbf{s}'}{|\mathbf{r}-\mathbf{s}'|^3}\cdot\mathbf{e}_r\,dS'$$
$$= \frac{\mu_0\sigma}{4\pi}\int_D \frac{\nabla_{r'}\times[\alpha(r')\mathbf{B}(\mathbf{r}')-\lambda\mathbf{A}(\mathbf{r}')]}{|\mathbf{r}-\mathbf{r}'|}\cdot\mathbf{e}_{r'}\frac{r'}{r}dV'. \tag{A1}$$

In the derivation of the last step in Eq. (A1) we have expressed $\mathbf{e}_r$ under the integrals by $(\mathbf{r}-\mathbf{r}')/r+(r'/r)\mathbf{e}_{r'}$, and we have used the fact that the triple product vanishes when $\mathbf{n}(\mathbf{s}')$ and $\mathbf{e}_{r'}$ coincide for $\mathbf{r}'=\mathbf{s}'$.

By virtue of Eq. (15), Eq. (A1) becomes

$$\mathbf{B}(\mathbf{r})\cdot\mathbf{e}_r = \frac{\mu_0\sigma}{4\pi}\int_D \frac{\nabla_{r'}\times[\alpha(r')\mathbf{B}(\mathbf{r}')]}{|\mathbf{r}-\mathbf{r}'|}\cdot\mathbf{e}_{r'}\frac{r'}{r}dV' - \frac{\mu_0\sigma\lambda}{4\pi}\int_D \frac{\mathbf{B}(\mathbf{r}')}{|\mathbf{r}-\mathbf{r}'|}\cdot\mathbf{e}_{r'}\frac{r'}{r}dV'. \tag{A2}$$

Noting that in Eq. (A2),

$$\nabla_{r'}\times[\alpha(r')\mathbf{B}(\mathbf{r}')] = -\mathbf{B}(\mathbf{r}')\times\nabla_{r'}\alpha(r') + \alpha(r')\nabla_{r'}\times\mathbf{B}(\mathbf{r}'), \tag{A3}$$

we see that the scalar product of the first term on the right-hand side with $\mathbf{e}_{r'}$ vanishes since the gradient of $\alpha(r')$ points in the $\mathbf{r}'$ direction, too. From Eqs. (34) and (35) we obtain

$$[\nabla_{r'}\times\mathbf{B}(\mathbf{r}')]\cdot\mathbf{e}_{r'} = \sum_{l',m'}\frac{l'(l'+1)}{r'^2}t_{l'm'}(r')Y_{l'm'}(\theta',\phi'). \tag{A4}$$

Taking Eqs. (A1), (A3), and (A4) together we find

$$\sum_{l,m}\frac{l(l+1)}{r^2}s_{lm}(r)Y_{lm}(\theta,\phi) = \frac{\mu_0\sigma}{4\pi r}\int_D \alpha(r')\sum_{l'm'}\frac{l'(l'+1)}{r'^2}t_{l'm'}(r')Y_{l'm'}(\theta',\phi')\frac{r'}{|\mathbf{r}-\mathbf{r}'|}dV' - \frac{\mu_0\sigma\lambda}{4\pi r}\int_D\sum_{l'm'}\frac{l'(l'+1)}{r'^2}s_{l'm'}(r')Y_{l'm'}(\theta',\phi')\frac{r'}{|\mathbf{r}-\mathbf{r}'|}dV'. \tag{A5}$$

After expressing the inverse distance according to Eq. (36), integrating on the right-hand side of Eq. (A5) over the primed angles, multiplying then both sides of Eq. (A5) with $Y^*_{lm}(\theta,\phi)$, and integrating over the nonprimed angles we obtain the first integral equation of our problem in the form

$$s_{lm}(r) = \frac{\mu_0\sigma}{2l+1}\left[\int_0^r \frac{r'^{l+1}}{r^l}\alpha(r')t_{lm}(r')dr' + \int_r^R \frac{r^{l+1}}{r'^l}\alpha(r')t_{lm}(r')dr' - \lambda\int_0^r \frac{r'^{l+1}}{r^l}s_{lm}(r')dr' - \lambda\int_r^R \frac{r^{l+1}}{r'^l}s_{lm}(r')dr'\right]. \tag{A6}$$

b. Electric potential at the boundary

For the determination of the electric potential at the boundary it is convenient to start from Eq. (24) for points **r** outside D. As for the last boundary integral in Eq. (24) we have

$$\frac{1}{4\pi}\int_S \varphi(\mathbf{s}')\mathbf{n}(\mathbf{s}')\cdot\frac{\mathbf{r}-\mathbf{s}'}{|\mathbf{r}-\mathbf{s}'|^3}dS' = \frac{1}{4\pi}\int_S \varphi(\mathbf{s}')\frac{\partial}{\partial s'}\frac{1}{|\mathbf{r}-\mathbf{s}'|}dS'$$
$$= \int_S \sum_{lm}\varphi_{lm}(R)Y_{lm}(\theta',\phi')\sum_{l'm'}\frac{1}{2l'+1}\frac{\partial}{\partial s'}\frac{s'^{l'}}{r^{l'+1}}Y^*_{l'm'}(\theta',\phi')Y_{l'm'}(\theta,\phi)dS' \tag{A7}$$

and thus

$$\lim_{\mathbf{r}\to\mathbf{s}}\frac{1}{4\pi}\int_S \varphi(\mathbf{s}')\mathbf{n}(\mathbf{s}')\cdot\frac{\mathbf{r}-\mathbf{s}'}{|\mathbf{r}-\mathbf{s}'|^3}dS' = \sum_{lm}\frac{l}{2l+1}\varphi_{lm}(R)Y_{lm}(\theta,\phi). \tag{A8}$$

For the evaluation of the volume integrals in Eq. (24) we can make the second one vanish by means of the Coulomb gauge $\boldsymbol{\nabla}\cdot\mathbf{A}$. For the first one, we use the alternative formulation Eq. (25). Taking B_r from Eq. (35), we find

$$\int_D \frac{\boldsymbol{\nabla}_{r'}\cdot[\alpha(r')\mathbf{B}(\mathbf{r}')]}{|\mathbf{r}-\mathbf{r}'|}dV' = \int_D \frac{d\alpha(r')}{dr'}\sum_{l'm'}\frac{l'(l'+1)}{r'^2}s_{l'm'}(r')Y_{l'm'}(\theta',\phi')\frac{1}{|\mathbf{r}-\mathbf{r}'|}dV' \tag{A9}$$

and thus

$$\lim_{\mathbf{r}\to\mathbf{s}}\frac{1}{4\pi}\int_D \frac{\boldsymbol{\nabla}_{r'}\cdot[\alpha(r')\mathbf{B}(\mathbf{r}')]}{|\mathbf{r}-\mathbf{r}'|}dV' = \sum_{lm}\frac{l(l+1)}{2l+1}Y_{lm}(\theta,\phi)\int_0^R \frac{r'^l}{R^{l+1}}\frac{d\alpha(r')}{dr'}s_{lm}(r')dr'. \tag{A10}$$

Analogously, we obtain, for the remaining boundary integrals in Eq. (24),

$$\lim_{\mathbf{r}\to\mathbf{s}}\frac{1}{4\pi}\int_S \mathbf{n}(\mathbf{s}')\cdot\frac{\alpha(s')\mathbf{B}(\mathbf{s}')-\lambda\mathbf{A}(\mathbf{s}')}{|\mathbf{r}-\mathbf{s}'|}dS' = \sum_{lm}\frac{l(l+1)}{2l+1}\frac{1}{R}[\alpha(R)s_{lm}(R)-\lambda s^A_{lm}(R)]Y_{lm}(\theta,\phi). \tag{A11}$$

Evaluating now Eq. (24) for $\mathbf{r}\to\mathbf{s}$ with the help of Eqs. (A8), (A10), and (A11) we find

$$\varphi_{lm}(R) = -(l+1)\int_0^R \frac{r'^l}{R^{l+1}}\frac{d\alpha(r')}{dr'}s_{lm}(r')dr' + \frac{l+1}{R}[\alpha(R)s_{lm}(R)-\lambda\, s^A_{lm}(R)]. \tag{A12}$$

This expression for $\varphi(R)$ will later be needed in the integral equation for $t_{lm}(r)$.

c. Vector potential at the boundary

From Eq. (27) and the fact that the curl of the magnetic field vanishes outside of D, we obtain

$$\int_D \frac{\nabla_{r'} \times \mathbf{B}(\mathbf{r}')}{|\mathbf{r}-\mathbf{r}'|} dV' = \int_{D+D'} \frac{\nabla_{r'} \times \mathbf{B}(\mathbf{r}')}{|\mathbf{r}-\mathbf{r}'|} dV', \quad \text{(A13)}$$

where D' denotes the outside region of D. Note that

$$\nabla_{r'} \times \frac{\mathbf{B}(\mathbf{r}')}{|\mathbf{r}-\mathbf{r}'|} = \nabla_{r'} \frac{1}{|\mathbf{r}-\mathbf{r}'|} \times \mathbf{B}(\mathbf{r}') + \frac{1}{|\mathbf{r}-\mathbf{r}'|} \nabla_{r'} \times \mathbf{B}(\mathbf{r}'). \quad \text{(A14)}$$

The application of this equation on the right-hand side of Eq. (A13) leads to

$$\int_D \frac{\nabla_{r'} \times \mathbf{B}(\mathbf{r}')}{|\mathbf{r}-\mathbf{r}'|} dV' = \int_{D+D'} \nabla_{r'} \times \frac{\mathbf{B}(\mathbf{r}')}{|\mathbf{r}-\mathbf{r}'|} dV' - \int_{D+D'} \nabla_{r'} \frac{1}{|\mathbf{r}-\mathbf{r}'|} \times \mathbf{B}(\mathbf{r}') dV'. \quad \text{(A15)}$$

Applying Gauss' theorem, we have

$$\int_D \frac{\nabla_{r'} \times \mathbf{B}(\mathbf{r}')}{|\mathbf{r}-\mathbf{r}'|} dV' = \int_{S_\infty} \mathbf{n}(\mathbf{s}') \times \frac{\mathbf{B}(\mathbf{r}')}{|\mathbf{r}-\mathbf{r}'|} dS' - \int_{D+D'} \frac{\mathbf{r}-\mathbf{r}'}{|\mathbf{r}-\mathbf{r}'|^3} \times \mathbf{B}(\mathbf{r}') dV'. \quad \text{(A16)}$$

Equation (3) allows us to conclude that the surficial integration on the RHS of this equation vanishes. Therefore, after taking the scalar product of both sides of Eq. (A16) with the unit vector $\mathbf{e}_r$, we obtain

$$\int_D \frac{\nabla_{r'} \times \mathbf{B}(\mathbf{r}')}{|\mathbf{r}-\mathbf{r}'|} \cdot \mathbf{e}_r dV' = -\int_{D+D'} \nabla_{r'} \frac{1}{|\mathbf{r}-\mathbf{r}'|} \times \mathbf{B}(\mathbf{r}') \cdot \mathbf{e}_{r'} \frac{r'}{r} dV'. \quad \text{(A17)}$$

In the derivation of this equation, the relation $\mathbf{e}_r = (\mathbf{r}-\mathbf{r}')/r + (r'/r)\mathbf{e}_{r'}$ has been used again. Applying Eq. (A14) again we have

$$\int_D \frac{\nabla_{r'} \times \mathbf{B}(\mathbf{r}')}{|\mathbf{r}-\mathbf{r}'|} \cdot \mathbf{e}_r dV' = \int_D \frac{\nabla_{r'} \times \mathbf{B}(\mathbf{r}')}{|\mathbf{r}-\mathbf{r}'|} \cdot \mathbf{e}_{r'} \frac{r'}{r} dV' - \int_{D+D'} \nabla_{r'} \times \frac{\mathbf{B}(\mathbf{r}')}{|\mathbf{r}-\mathbf{r}'|} \cdot \mathbf{e}_{r'} \frac{r'}{r} dV'. \quad \text{(A18)}$$

The second term on the RHS of Eq. (A18) can be shown to vanish, so we conclude that

$$\mathbf{A}(\mathbf{r}) \cdot \mathbf{e}_r = \frac{1}{4\pi} \int_D \frac{\nabla_{r'} \times \mathbf{B}(\mathbf{r}')}{|\mathbf{r}-\mathbf{r}'|} \cdot \mathbf{e}_{r'} \frac{r'}{r} dV'. \quad \text{(A19)}$$

Hence we obtain

$$s^A_{lm}(r) = \frac{1}{2l+1} \left(\int_0^r \frac{r'^{l+1}}{r^l} t_{lm}(r') dr' + \int_r^R \frac{r^{l+1}}{r'^l} t_{lm}(r') dr' \right). \quad \text{(A20)}$$

Particularly, when $r=R$ in the above equation, we have

$$s^A_{lm}(R) = \frac{1}{2l+1} \int_0^R \frac{r'^{l+1}}{R^l} t_{lm}(r') dr'. \quad \text{(A21)}$$

As we will see, there is no need to calculate the corresponding expression for $t^A_{lm}(r)$.

d. Radial integral equation for $t_{lm}(r)$

We take now the *curl* of both sides of Eq. (20), thus obtaining

$$\nabla_r \times \mathbf{B}(\mathbf{r}) = \frac{\mu_0 \sigma}{4\pi} \left[\nabla_r \times \nabla_r \times \int_D \frac{\alpha(r')\mathbf{B}(\mathbf{r}') - \lambda \mathbf{A}(\mathbf{r}')}{|\mathbf{r}-\mathbf{r}'|} dV' - \nabla_r \times \int_S \varphi(\mathbf{s}') \mathbf{n}(\mathbf{s}') \times \frac{\mathbf{r}-\mathbf{s}'}{|\mathbf{r}-\mathbf{s}'|^3} dS' \right]. \quad \text{(A22)}$$

Considering first the case $r \leqslant R$ we take on both sides of Eq. (A22) the scalar product with $\mathbf{e}_r$. We note that

$$\mathbf{e}_r \cdot \left(\nabla_r \times \nabla_r \times \int_D \frac{\alpha(r')\mathbf{B}(\mathbf{r}') - \lambda \mathbf{A}(\mathbf{r}')}{|\mathbf{r}-\mathbf{r}'|} dV' \right) = \mathbf{e}_r \cdot \left((\nabla_r \nabla_r \cdot - \Delta_r) \int_D \frac{\alpha(r')\mathbf{B}(\mathbf{r}') - \lambda \mathbf{A}(\mathbf{r}')}{|\mathbf{r}-\mathbf{r}'|} dV' \right) = \frac{\partial}{\partial r} \int_D \frac{\nabla_{r'} \cdot [\alpha(r')\mathbf{B}(\mathbf{r}')]}{|\mathbf{r}-\mathbf{r}'|} dV' - \frac{\partial}{\partial r} \int_S \mathbf{n}(\mathbf{s}') \cdot \frac{\alpha(s')\mathbf{B}(\mathbf{s}') - \lambda \mathbf{A}(\mathbf{s}')}{|\mathbf{r}-\mathbf{s}'|} dS' + 4\pi [\alpha(r) B_r(r) - \lambda A_r(r)], \quad \text{(A23)}$$

where we have used the identity $\Delta_r |\mathbf{r}-\mathbf{r}'|^{-1} = -4\pi\delta(\mathbf{r}-\mathbf{r}')$ and the Coulomb gauge $\nabla \cdot \mathbf{A} = 0$. The two integrals on the third RHS line of Eq. (A23) were already treated in Appendix A 1. Concerning the boundary integral in Eq. (A22) over the electric potential we note that

$$\mathbf{e}_r \cdot \left[\boldsymbol{\nabla}_r \times \left(\mathbf{n}(\mathbf{s}') \times \frac{\mathbf{r}-\mathbf{s}'}{|\mathbf{r}-\mathbf{s}'|^3} \right) \right] = -\frac{\partial^2}{\partial r \, \partial s'} \frac{1}{|\mathbf{r}-\mathbf{s}'|}. \tag{A24}$$

Putting everything together we obtain

$$[\boldsymbol{\nabla}_r \times \mathbf{B}(\mathbf{r})] \cdot \mathbf{e}_r = \mu_0 \sigma [\alpha(r) B_r(\mathbf{r}) - \lambda A_r(r)] + \frac{\mu_0 \sigma}{4\pi} \left[\frac{\partial}{\partial r} \int_D \frac{d\alpha(r')}{dr'} B_r(\mathbf{r}') \frac{1}{|\mathbf{r}-\mathbf{r}'|} dV' - \frac{\partial}{\partial r} \int_S \frac{\alpha(s') B_r(\mathbf{s}') - \lambda A_r(\mathbf{s}')}{|\mathbf{r}-\mathbf{s}'|} dS' + \int_S \varphi(\mathbf{s}') \frac{\partial^2}{\partial r \, \partial s'} \frac{1}{|\mathbf{r}-\mathbf{s}'|} dS' \right].$$

Representing now the left-hand side according to Eq. (A4), applying Eq. (36), and integrating both sides over the angles we obtain

$$t_{lm}(r) = \mu_0 \sigma \left[\alpha(r) s_{lm}(r) - \lambda s^A_{lm}(r) - \frac{l+1}{2l+1} \int_0^r \frac{d\alpha(r')}{dr'} s_{lm}(r') \frac{r'^l}{r^l} dr' + \frac{l}{2l+1} \int_r^R \frac{d\alpha(r')}{dr'} s_{lm}(r') \frac{r^{l+1}}{r'^{l+1}} dr' - \frac{l}{2l+1} \frac{r^{l+1}}{R^{l+1}} [\alpha(R) s_{lm}(R) - \lambda \, s^A_{lm}(R)] - \frac{1}{2l+1} \varphi_{lm}(R) \frac{r^{l+1}}{R^l} \right]. \tag{A25}$$

Substituting Eqs. (A12) and (A21) into Eq. (A25) leads to

$$t_{lm}(r) = \mu_0 \sigma \left[\alpha(r) s_{lm}(r) - \frac{l+1}{2l+1} \int_0^r \frac{d\alpha(r')}{dr'} s_{lm}(r') \frac{r'^l}{r^l} dr' + \frac{l}{2l+1} \int_r^R \frac{d\alpha(r')}{dr'} s_{lm}(r') \frac{r^{l+1}}{r'^{l+1}} dr' + \frac{l+1}{2l+1} \frac{r^{l+1}}{R^{2l+1}} \int_0^R r'^l \frac{d\alpha(r')}{dr'} s_{lm}(r') dr' + \frac{\lambda}{2l+1} \frac{r^{l+1}}{R^{2l+1}} \int_0^R r'^{l+1} t_{lm}(r') dr' - \frac{\lambda}{2l+1} \int_0^r \frac{r'^{l+1}}{r^l} t_{lm}(r') dr' - \frac{\lambda}{2l+1} \int_r^R \frac{r^{l+1}}{r'^l} t_{lm}(r') dr' - \frac{r^{l+1}}{R^{l+1}} \alpha(R) s_{lm}(R) \right]. \tag{A26}$$

This is the second radial integral equation for our problem. Therefore, the spherically symmetric α^2 dynamo model is reduced to the two coupled integral equations (A6) and (A26).

2. Derivation from the radial differential equation system using a Green's function method

In this part, we give an alternative approach to establish the integral equations (37) and (38), starting with the radial differential equation problem (39)–(41).

First, we derive the Green's function $G_s(r, r_0)$, corresponding to Eq. (39). This Green's function satisfies

$$\frac{\partial^2 G_s}{\partial r^2} - \frac{l(l+1)}{r^2} G_s = \delta(r - r_0), \tag{A27}$$

$$G_s|_{r=0} = 0, \tag{A28}$$

$$R \left. \frac{\partial G_s}{\partial r} \right|_{r=R} + l \, G_s|_{r=R} = 0. \tag{A29}$$

According to the construction method of Green's functions ([40], p. 355), we obtain $G_s(r, r_0)$ in the following form:

$$G_s(r, r_0) = \begin{cases} -\frac{1}{2l+1} r_0^{-l} r^{l+1}, & r \leqslant r_0, \\ -\frac{1}{2l+1} r_0^{l+1} r^{-l}, & r \geqslant r_0. \end{cases} \tag{A30}$$

As for Eq. (40), we first rewrite it in the form

$$\frac{1}{\mu_0 \sigma} \frac{d^2 F}{dr^2} - \frac{1}{\mu_0 \sigma} \frac{l(l+1)}{r^2} F + \frac{d}{dr} \left(\frac{d\alpha}{dr} s_{lm} \right) - \mu_0 \sigma \lambda t_{lm} = 0, \tag{A31}$$

where $F = t_{lm} - \mu_0 \sigma \alpha s_{lm}$. This differential equation problem for t_{lm} can be split into two problems. One of them reads

$$\frac{d^2 F_1}{dr^2} - \frac{l(l+1)}{r^2} F_1 + \mu_0 \sigma \frac{d}{dr} \left(s_{lm} \frac{d\alpha}{dr} \right) - \mu_0 \sigma \lambda t_{lm} = 0,$$

$$F_1|_{r=R} = 0. \tag{A32}$$

The other is

$$\frac{d^2 F_2}{dr^2} - \frac{l(l+1)}{r^2} F_2 = 0,$$

$$F_2|_{r=R} = -\mu_0\sigma\alpha(R)s_{lm}(R). \tag{A33}$$

For the differential equation problem (A32), applying the construction method of Green's function [40] again, we obtain its Green's function in the form

$$G_t(r,r_0) = \begin{cases} \dfrac{1}{R^{2l+1}(2l+1)}(r_0^{l+1} - R^{2l+1}r_0^{-l})r^{l+1}, & r \leqslant r_0, \\ \dfrac{1}{R^{2l+1}(2l+1)}(r^{l+1} - R^{2l+1}r^{-l})r_0^{l+1}, & r \geqslant r_0, \end{cases} \tag{A34}$$

which satisfies

$$\frac{\partial^2 G_t}{\partial r^2} - \frac{l(l+1)}{r^2}G_t = 0, \tag{A35}$$

$$G_t|_{r=0} = 0, \tag{A36}$$

$$G_t|_{r=R} = 0. \tag{A37}$$

As for the differential equation problem (A33), the solution can be expressed as

$$F_2 = -\frac{\mu_0\sigma}{R^{l+1}}\alpha(R)s_{lm}(R)r^{l+1}. \tag{A38}$$

Then the superposition theorem of the linear problems allows us to obtain the following integral equations for s_{lm} and t_{lm}:

$$s_{lm}(r) = -\int_0^R G_s(r,r_0)\mu_0\sigma\alpha(r_0)t_{lm}(r_0)dr_0 + \mu_0\sigma\lambda\int_0^R G_s(r,r_0)s_{lm}(r_0)dr_0, \tag{A39}$$

$$t_{lm}(r) = \mu_0\sigma\alpha(r)s_{lm}(r) - \int_0^R \mu_0\sigma\frac{d}{dr_0}\left(s_{lm}(r_0)\frac{d\alpha(r_0)}{dr_0}\right)G_t(r,r_0)dr_0 + \lambda\mu_0\sigma\int_0^R G_t(r,r_0)t_{lm}(r_0)dr_0 - \frac{r^{l+1}}{R^{l+1}}\mu_0\sigma\alpha(R)s_{lm}(R). \tag{A40}$$

Integrating by parts the terms containing derivatives of s_{lm} in Eq. (A40), we obtain

$$s_{lm}(r) = -\int_0^R G_s(r,r_0)\mu_0\sigma\alpha(r_0)t_{lm}(r_0)dr_0 + \mu_0\sigma\lambda\int_0^R G_s(r,r_0)s_{lm}(r_0)dr_0, \tag{A41}$$

$$t_{lm}(r) = \mu_0\sigma\alpha(r)s_{lm}(r) + \int_0^R \mu_0\sigma\frac{d\alpha(r_0)}{dr_0}s_{lm}(r_0)\frac{\partial G_t(r,r_0)}{\partial r_0}dr_0 + \lambda\mu_0\sigma\int_0^R G_t(r,r_0)t_{lm}(r_0)dr_0 - \frac{r^{l+1}}{R^{l+1}}\mu_0\sigma\alpha(R)s_{lm}(R). \tag{A42}$$

Therefore, we have obtained the same integral equations as expressed in Eqs. (37) and (38).

APPENDIX B: SOME NOTATIONS

In this appendix, we define the constants c_i that are used in Sec. IV. These are

$$c_1 = -\frac{L\beta(\beta+1)}{N_\gamma},$$

$$c_2 = -\frac{L\alpha(\alpha+1)}{N_\gamma},$$

$$c_3 = -\frac{K}{2N_\gamma}\alpha(\alpha+1)[\alpha(\alpha+1) - \beta(\beta+1) - \gamma(\gamma+1)],$$

$$c_4 = -\frac{K}{2N_\gamma}\beta(\beta+1)[\alpha(\alpha+1) - \beta(\beta+1) + \gamma(\gamma+1)],$$

$$c_5 = -\frac{L\gamma(\gamma+1)}{N_\gamma},$$

$$c_6 = -\frac{K}{2N_\gamma}\{\beta(\beta+1)[\alpha(\alpha+1) - \beta(\beta+1) + \gamma(\gamma+1)] + \gamma(\gamma+1)[\alpha(\alpha+1) + \beta(\beta+1) - \gamma(\gamma+1)]\},$$

$$c_7 = -\frac{K}{2N_\gamma}\beta(\beta+1)[\alpha(\alpha+1) - \beta(\beta+1) + \gamma(\gamma+1)],$$

$$c_8 = \frac{K}{2N_\gamma}\alpha(\alpha+1)[-\alpha(\alpha+1) + \beta(\beta+1) + \gamma(\gamma+1)],$$

$$c_9 = \frac{K}{2N_\gamma}\gamma(\gamma+1)[\alpha(\alpha+1) + \beta(\beta+1) - \gamma(\gamma+1)],$$

$$c_{10} = \frac{L}{N_\gamma}\alpha(\alpha+1),$$

$$c_{11} = \frac{L}{N_\gamma}[\alpha(\alpha+1) + \beta(\beta+1) - \gamma(\gamma+1)],$$

$$c_{12} = -\frac{2L}{N_\gamma}\alpha(\alpha+1),$$

$$c_{13} = \frac{L}{N_\gamma}\beta(\beta+1). \tag{B1}$$

In Eq. (B1) we have used the expressions for the Adams-Gaunt and Elsasser integrals,

$$K = \int_0^{2\pi}\int_0^{\pi} Y_\alpha Y_\beta Y_\gamma \sin\theta d\theta d\varphi,$$

$$L = \int_0^{2\pi}\int_0^{\pi} Y_\alpha\left(\frac{\partial Y_\beta}{\partial\theta}\frac{\partial Y_\gamma}{\partial\varphi} - \frac{\partial Y_\beta}{\partial\varphi}\frac{\partial Y_\gamma}{\partial\theta}\right)d\theta d\varphi, \tag{B2}$$

and the normalization factor

$$N_\gamma = \begin{cases} \dfrac{2\pi\gamma(\gamma+1)}{2\gamma+1}\dfrac{(\gamma+m)!}{(\gamma-m)!}, & m \neq 0, \\ \dfrac{4\pi\gamma(\gamma+1)}{2\gamma+1}, & m = 0. \end{cases}$$

[1] F. Krause and K.-H. Rädler, *Mean-field Magnetohydrodynamics and Dynamo Theory* (Akademie-Verlag, Berlin, 1980).
[2] H. K. Moffatt, *Magnetic Field Generation in Electrically Conducting Fluids* (Cambridge University Press, Cambridge, England, 1978).
[3] A. Gailitis *et al.*, Phys. Rev. Lett. **84**, 4365 (2000).
[4] U. Müller and R. Stieglitz, Naturwissenschaften **87**, 381 (2000).
[5] A. Gailitis *et al.*, Phys. Rev. Lett. **86**, 3024 (2002).
[6] R. Stieglitz and U. Müller, Phys. Fluids **13**, 561 (2001).
[7] A. Gailitis, O. Lielausis, E. Platacis, G. Gerbeth, and F. Stefani, Rev. Mod. Phys. **74**, 973 (2002).
[8] A. Brandenburg, Å. Nordlund, R. F. Stein, and U. Torkelsson, Astrophys. J. **446**, 741 (1995).
[9] G. Rüdiger and Y. Zhang, Astron. Astrophys. **378**, 302 (2001).
[10] K.-H. Rädler, E. Apstein, M. Rheinhardt, and M. Schüler, Stud. Geophys. Geod. **42**, 224 (1998).
[11] K.-H. Rädler, M. Rheinhardt, E. Apstein, and H. Fuchs, Nonlinear Processes Geophys. **9**, 171 (2002).
[12] F. Stefani, G. Gerbeth, and A. Gailitis, in *Transfer Phenomena in Magnetohydrodynamics and Electroconducting Flows*, edited by A. Alemany, Ph. Marty, and J.-P. Thibault (Kluwer, Dordrecht, 1999), p. 31.
[13] A. Gailitis, Magnetohydrodynamics (N.Y.) **6**(1), 14 (1970).
[14] A. Gailitis and Ya. Freiberg, Magnetohydrodynamics (N.Y.) **10**(1), 26 (1974).
[15] Ya. Freiberg, Magnetohydrodynamics (N.Y.) **11**(3), 269 (1975).
[16] W. Dobler and K.-H. Rädler, Geophys. Astrophys. Fluid Dyn. **89**, 45 (1998).
[17] P. H. Roberts, *An Introduction to Magnetohydrodynamics* (Elsevier, New York, 1967).
[18] F. Stefani, G. Gerbeth, and K.-H. Rädler, Astron. Nachr. **321**, 65 (2000).
[19] F. Krause and M. Steenbeck, Z. Naturforsch. A **22**, 671 (1967).
[20] M. Xu, F. Stefani, and G. Gerbeth, J. Comput. Phys. **196**, 102 (2004).
[21] A. J. Meir and P. G. Schmidt, Appl. Math. Comput. **65**, 95 (1994).
[22] A. J. Meir and P. G. Schmidt, SIAM (Soc. Ind. Appl. Math.) J. Numer. Anal. **36**, 1304 (1999).
[23] A. Gailitis, O. Lielausis, E. Platacis, G. Gerbeth, and F. Stefani, Surv. Geophys. **24**, 247 (2003).
[24] F. Stefani and G. Gerbeth, Inverse Probl. **15**, 771 (1999).
[25] F. Stefani and G. Gerbeth, Inverse Probl. **16**, 1 (2000).
[26] F. Stefani and G. Gerbeth, Meas. Sci. Technol. **11**, 758 (2000).
[27] F. Stefani, Th. Gundrum, G. Gerbeth, U. Günther, and M. Xu, e-print physics/0312093.
[28] B. F. Farrell and P. J. Ioannou, Astrophys. J. **522**, 1079 (1999).
[29] B. F. Farrell and P. J. Ioannou, Astrophys. J. **522**, 1088 (1999).
[30] P. Livermore and A. Jackson, in *Computational Fluid and Solid Mechanics 2003*, edited by K.-J. Bathe (Elsevier, New York, 2003), p. 1004.
[31] F. Stefani and G. Gerbeth, Phys. Rev. E **67**, 027302 (2003).
[32] J. Cantarella, D. DeTurck, and H. Gluck, J. Math. Phys. **42**, 876 (2001).
[33] P. M. Morse and H. Feshbach, *Methods of Theoretical Physics* (McGraw-Hill, New York, 1953).
[34] K.-H. Rädler (unpublished).
[35] E. C. Bullard and H. Gellman, Philos. Trans. R. Soc. London, Ser. A **247**, 213 (1954).
[36] R. D. Gibson, P. H. Roberts, and S. Scott, in *The Application of Modern Physics to the Earth and Planetary Interiors*, edited by S. K. Runcorn (Wiley Interscience, New York, 1969), p. 577.
[37] M. L. Dudley and R. W. James, Proc. R. Soc. London, Ser. A **425**, 407 (1989).
[38] A. C. L. Barnard, I. M. Duck, M. S. Lynn, and W. P. Timlake, Biophys. J. **7**, 463 (1967).
[39] M. Hämäläinen, R. Hari, R. J. Ilmoniemi, J. Knuutila, and O. V. Lounasmaa, Rev. Mod. Phys. **65**, 413 (1993).
[40] R. Courant and D. Hilbert, *Methods of Mathematical Physics* (Interscience, New York, 1953).